SAND2020-0086C

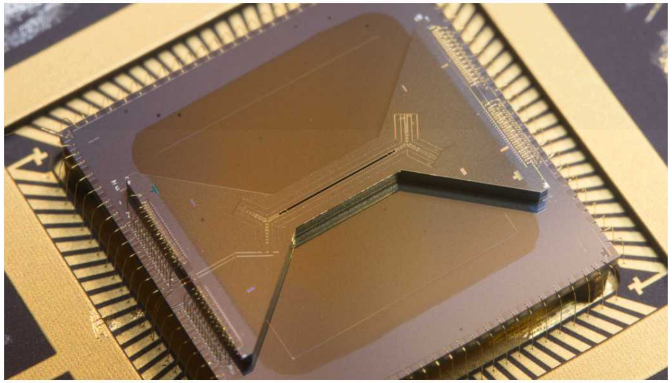

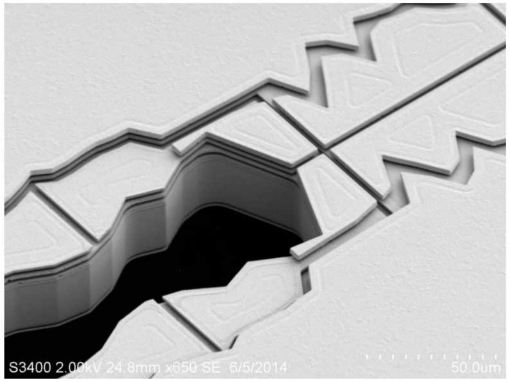

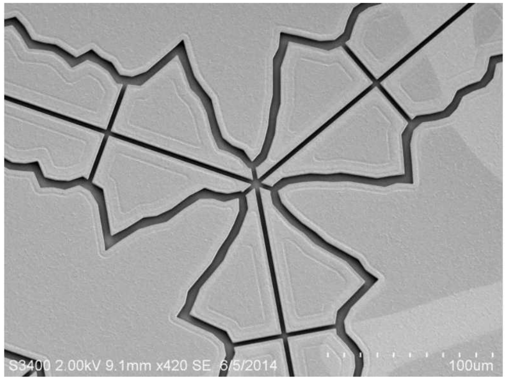

Surface ion traps for quantum computing

ASPE 2020 Winter Topical Meeting (January 17, 2020)

Dr. Daniel Stick

Sandia National Laboratories is a multimission laboratory managed and operated by National Technology & Engineering Solutions of Sandia, LLC, a wholly owned subsidiary of Honeywell International Inc., for the U.S. Department of Energy's National Nuclear Security Administration under contract DE-NA0003525.

Outline

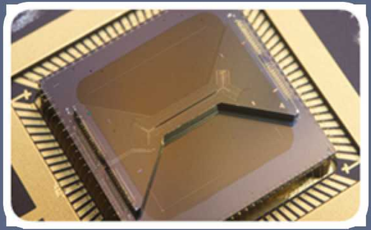

Ion trapology

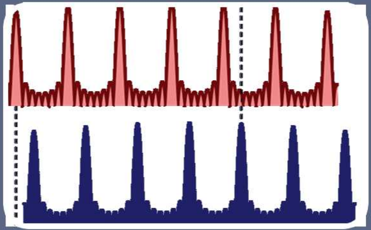

Classical characterization

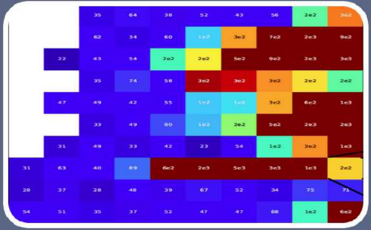

Quantum characterization

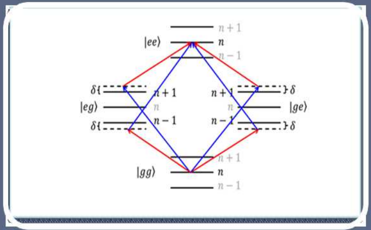

Specialized devices and Future directions

Outline

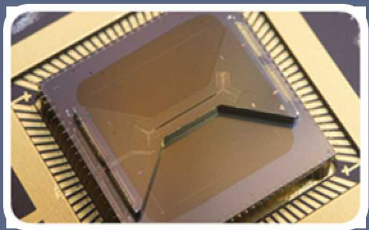

Ion trapology

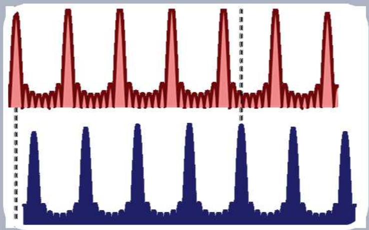

Classical characterization

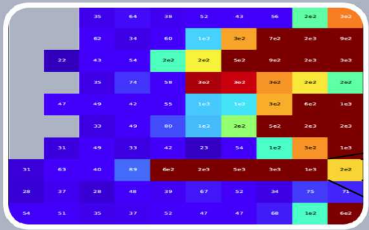

Quantum characterization

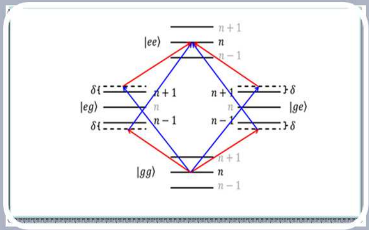

Specialized devices and Future directions

Advantages/Challenges vs 3D

Advantages

- More manufacturable ("scalable")
- Consistent geometry -> consistent behavior
- Greater field control (more electrodes)
- 2D geometry
- Integration of other technologies (waveguides, detectors, filters…)
- Laser access

Challenges

- Low depth (ion lifetime), anharmonicities in potential
- Proximity to surface (charging, heating)
- Delicate (dust, voltage)
- Capacitance

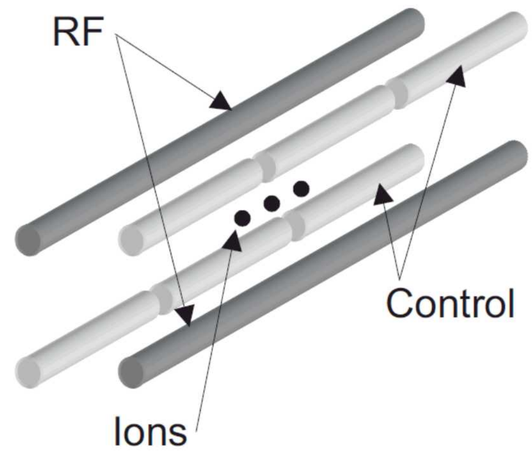

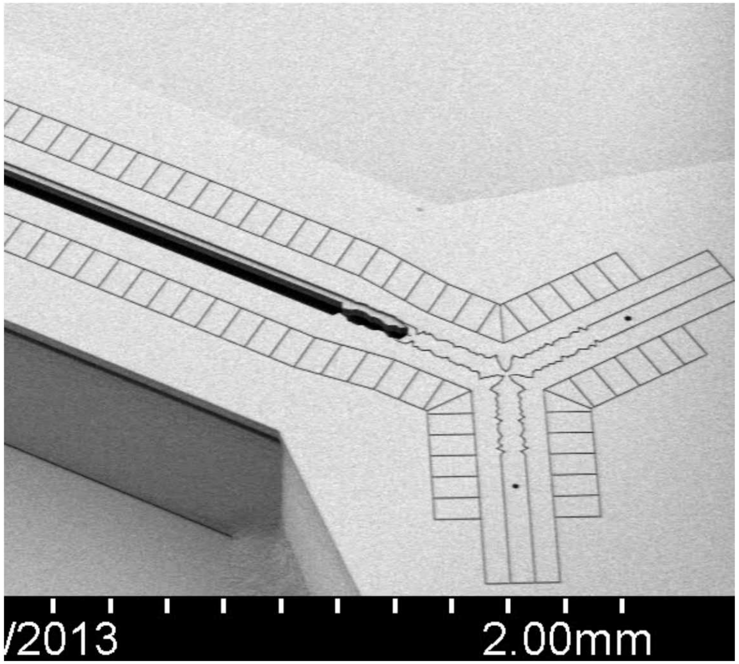

Capabilities & Requirements

Essential capabilities

- Store ions for long periods of time (hours)
- Move ions to achieve 2D connectivity
- Support high fidelity operations
- Uniform performance

Derived requirements

- Voltage breakdown >300 V @ ~50 MHz
- Backside loading hole
- Multi-level lead routing for accessing interior electrodes
- Standardization [lithographically defined electrodes]
- Overhung electrodes
- High optical access [high NA delivery and collection optics]

Quantum CCD

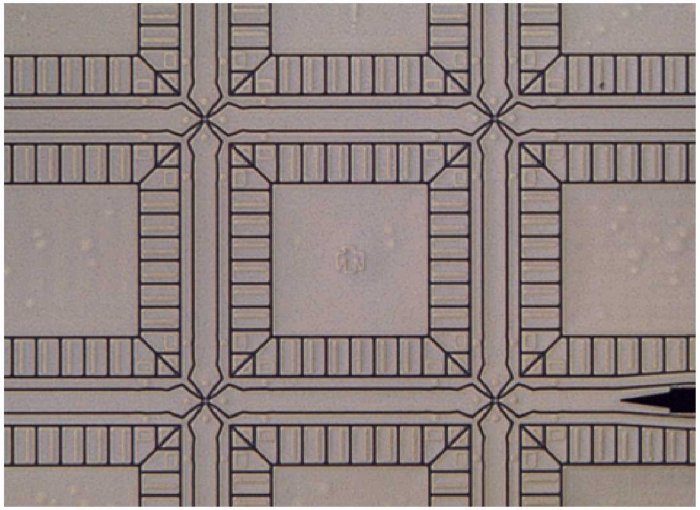

MUSIQC architecture

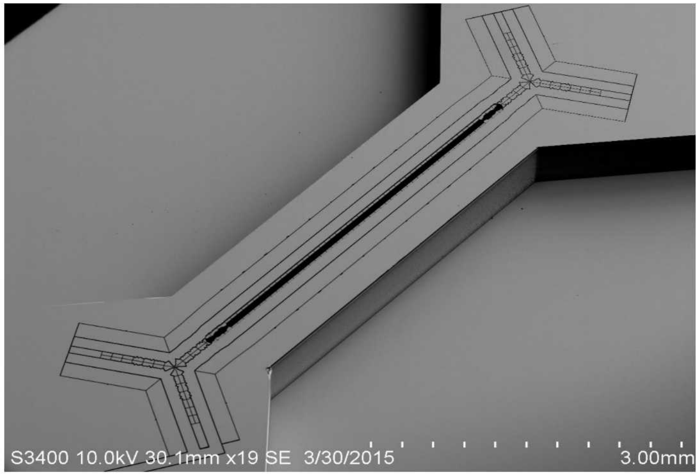

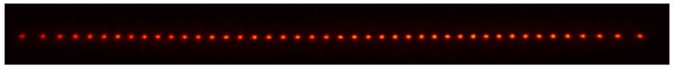

Voltage application

Trapping potential

- Axial frequency: 500 kHz [<5 V]
- Radial frequency: 2.8 MHz, 3.1 MHz [250 Vrf @ 40 MHz]

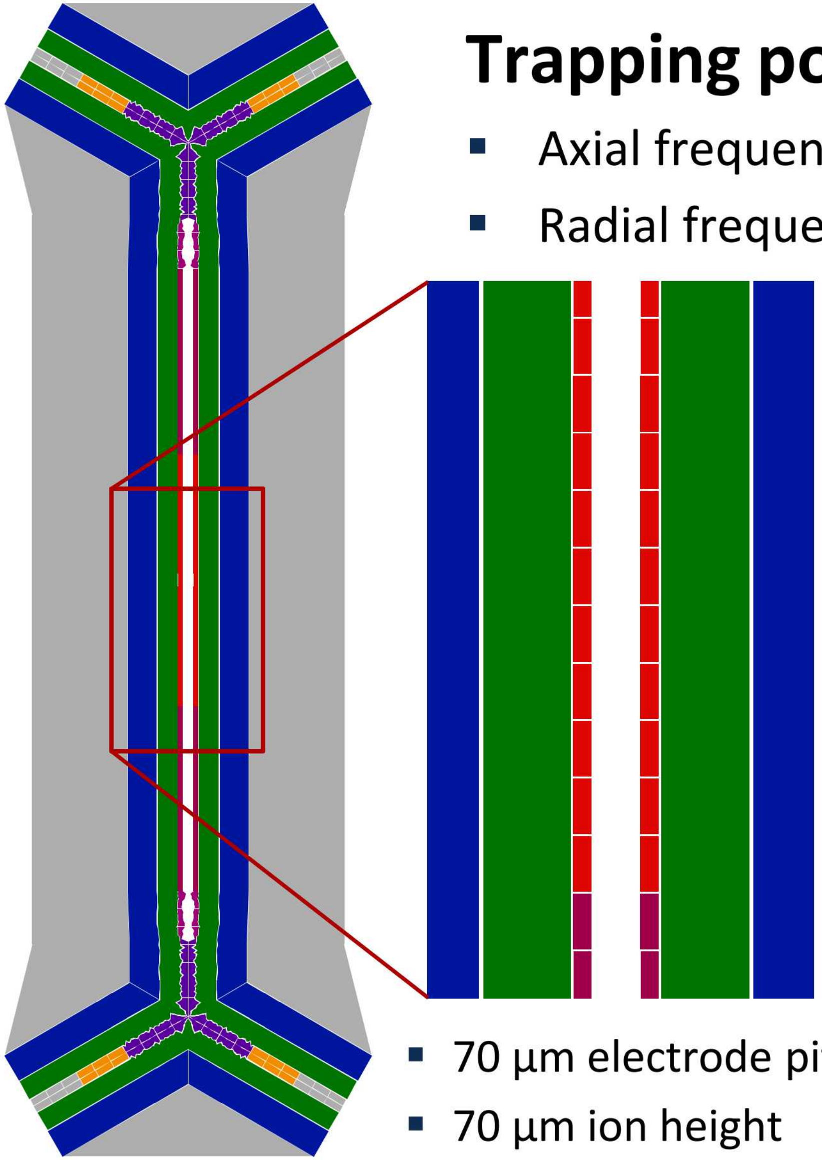

- 70 µm electrode pitch
- 70 µm ion height

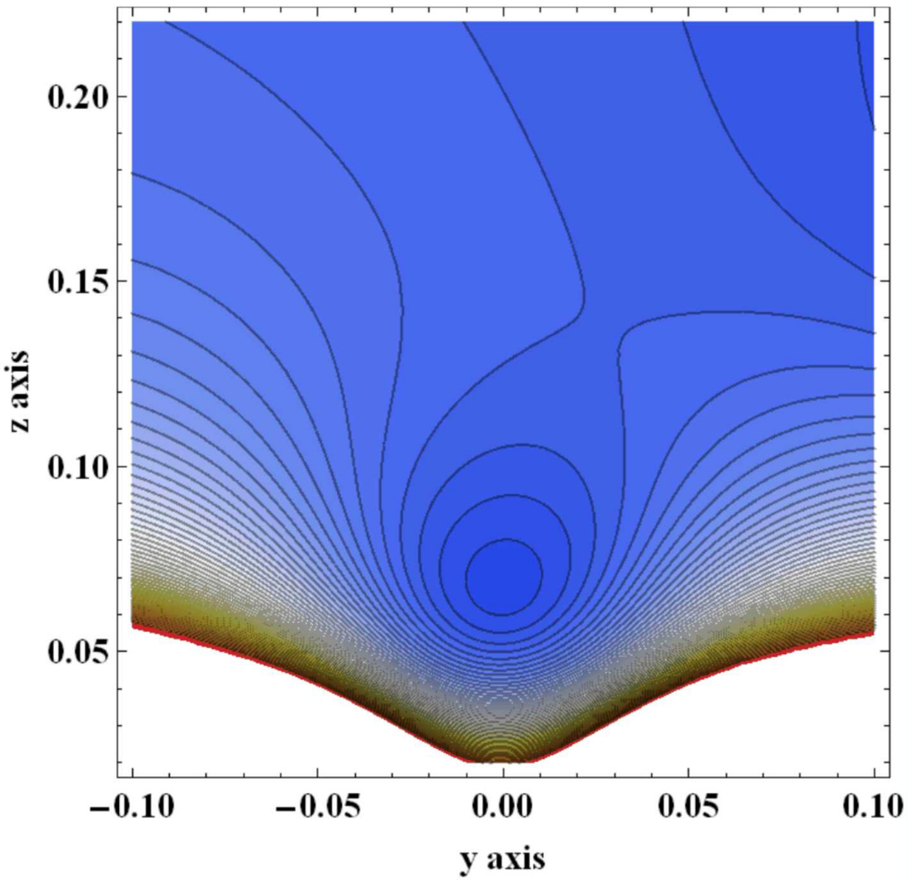

Multi-layer metallization

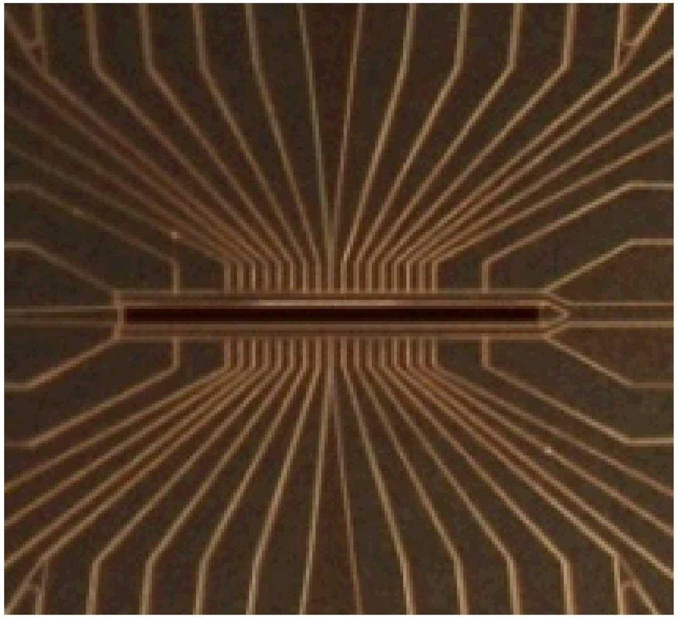

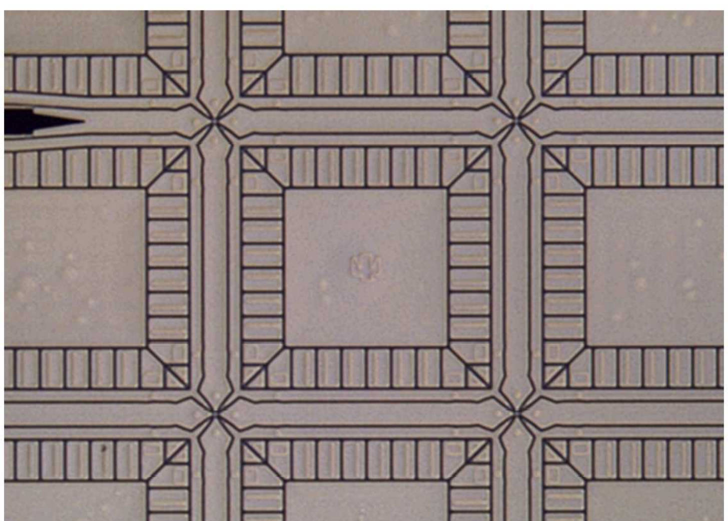

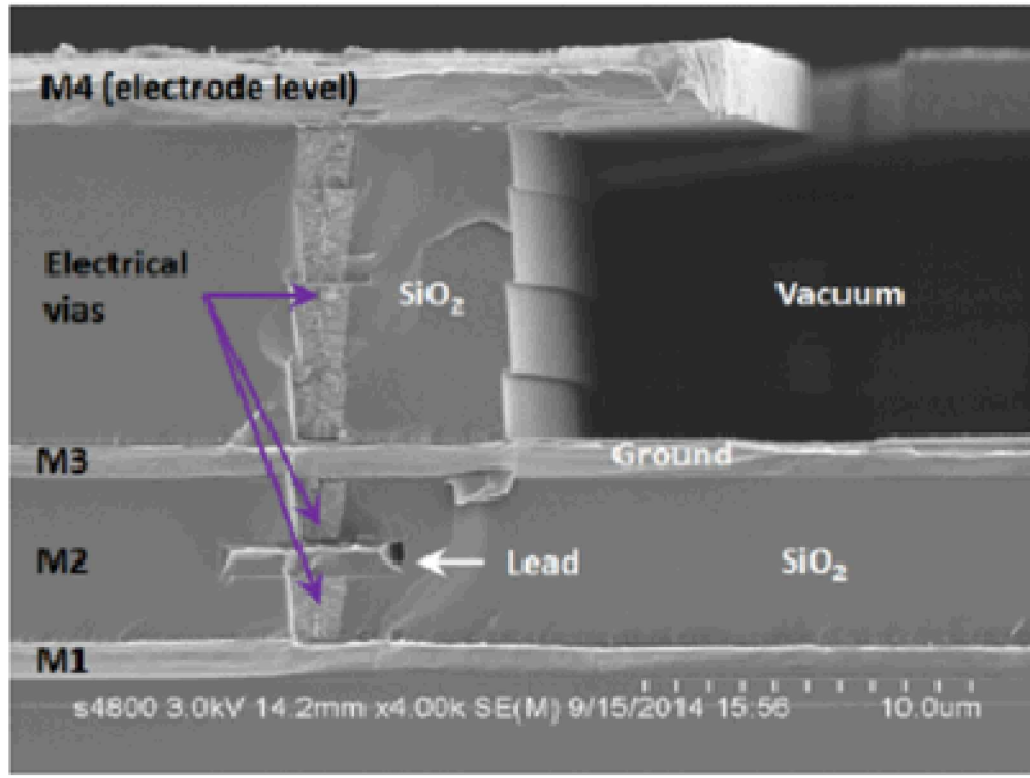

Trench capacitors & Loading holes

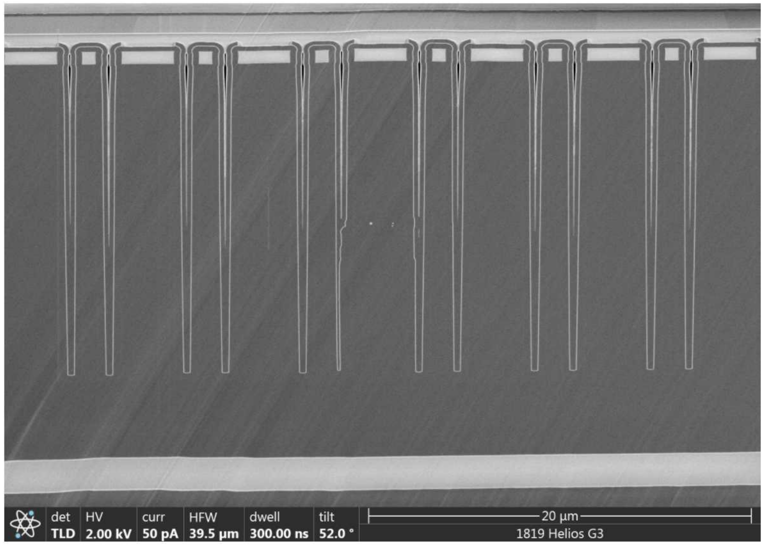

Interposer (current)

- 20V max voltage
- 1nF capacitance

On chip (future)

- 15V max voltage
- 200pF capacitance (but low inductance)
- Up to 200 capacitors can be located within the isthmus

50µm×80µm
modulation necessary

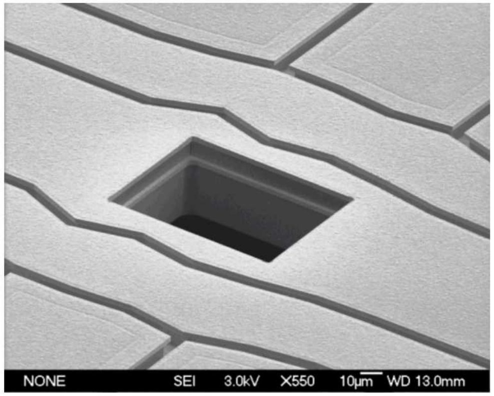

10µm hole
still perturbs the field

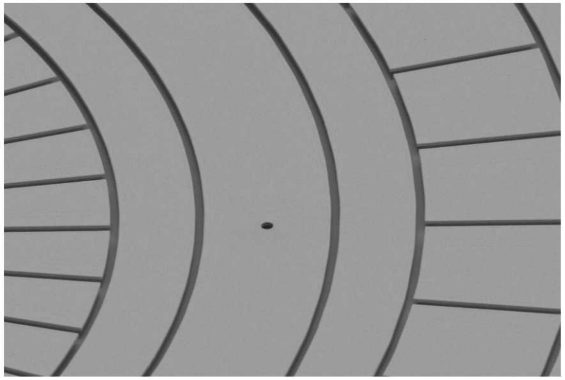

3µm×20µm

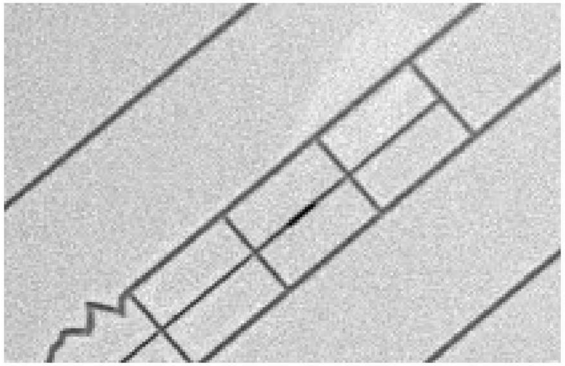

Optical access & integrated optics

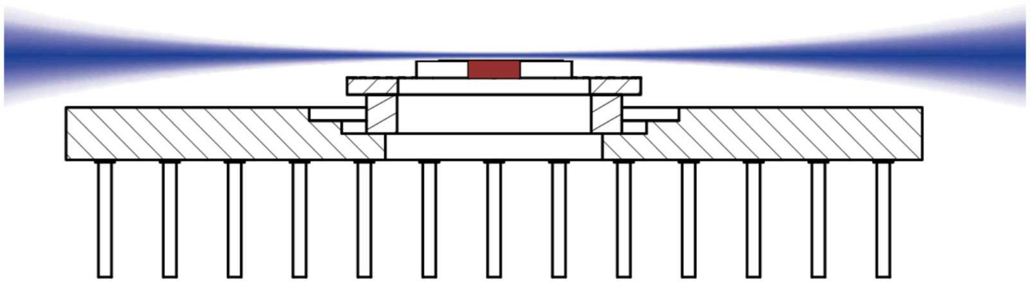

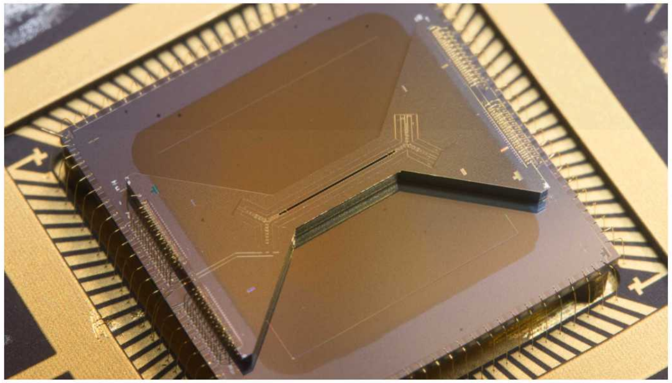

Can accommodate 4/2 um beam waist (369 nm)

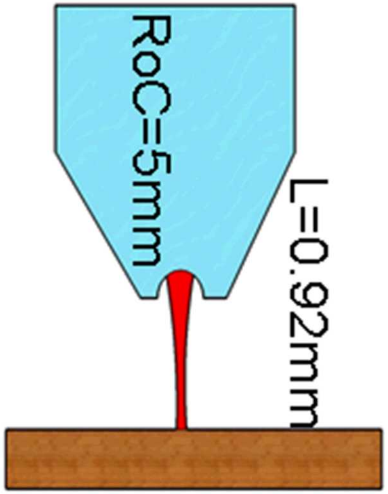

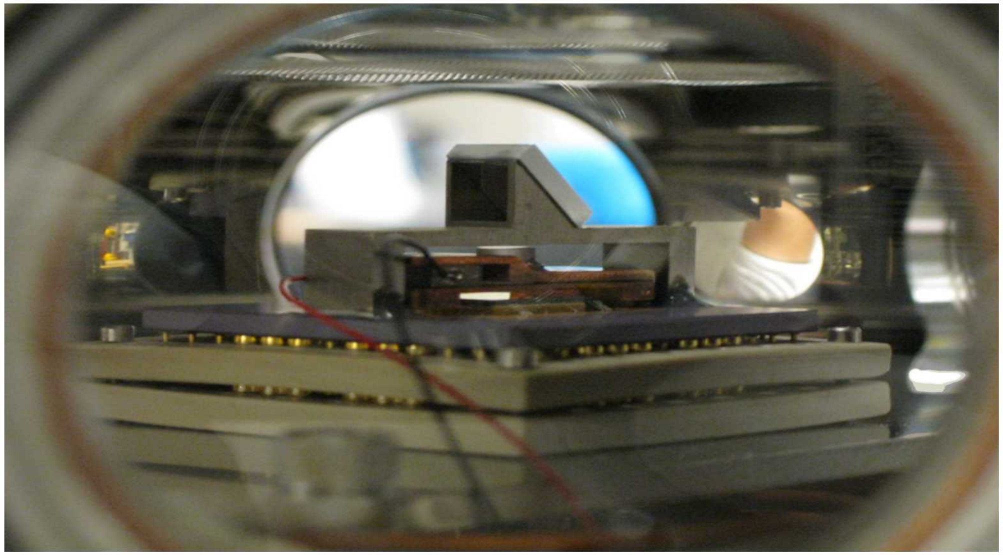

Some of Sandia's Traps

Y-junction traps

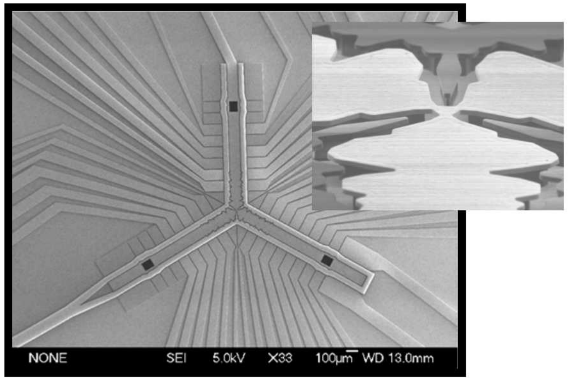

Circulator trap

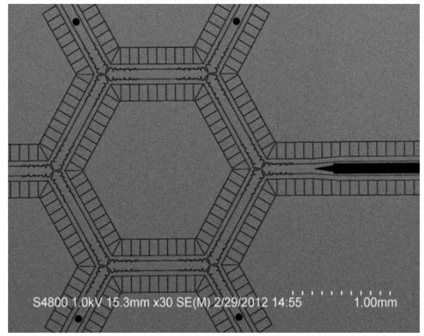

High Optical Access (HOA) trap

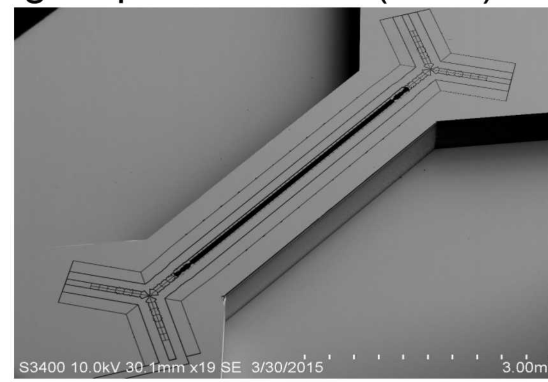

Ring trap:

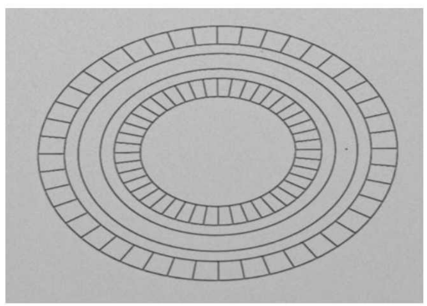

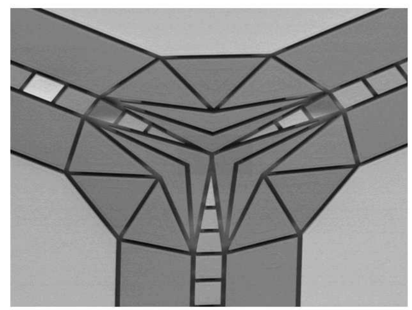

: Switchable RF trap

Stylus trap

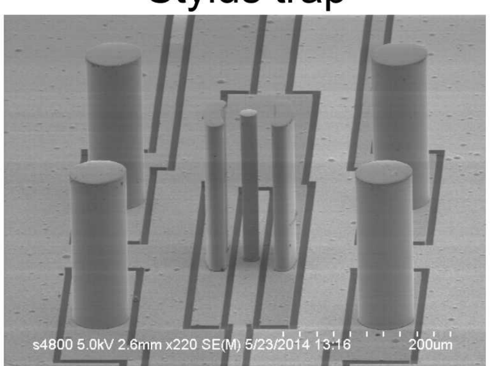

Microwave trap

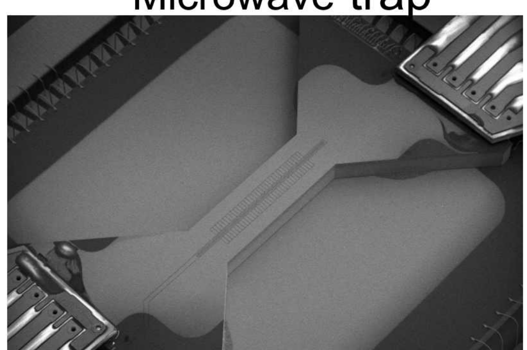

EPICS trap

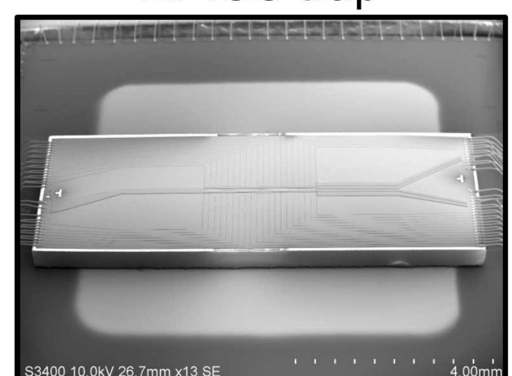

Outline

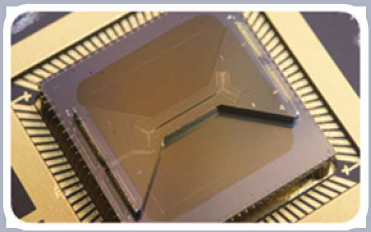

Ion trapology

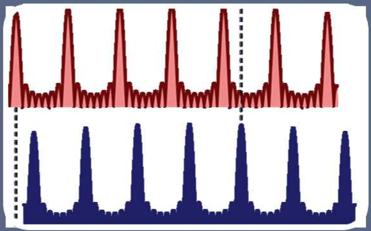

Classical characterization

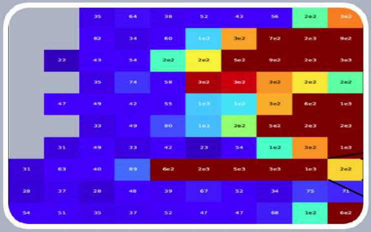

Quantum characterization

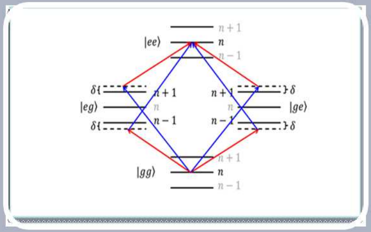

Specialized devices and Future directions

Heating

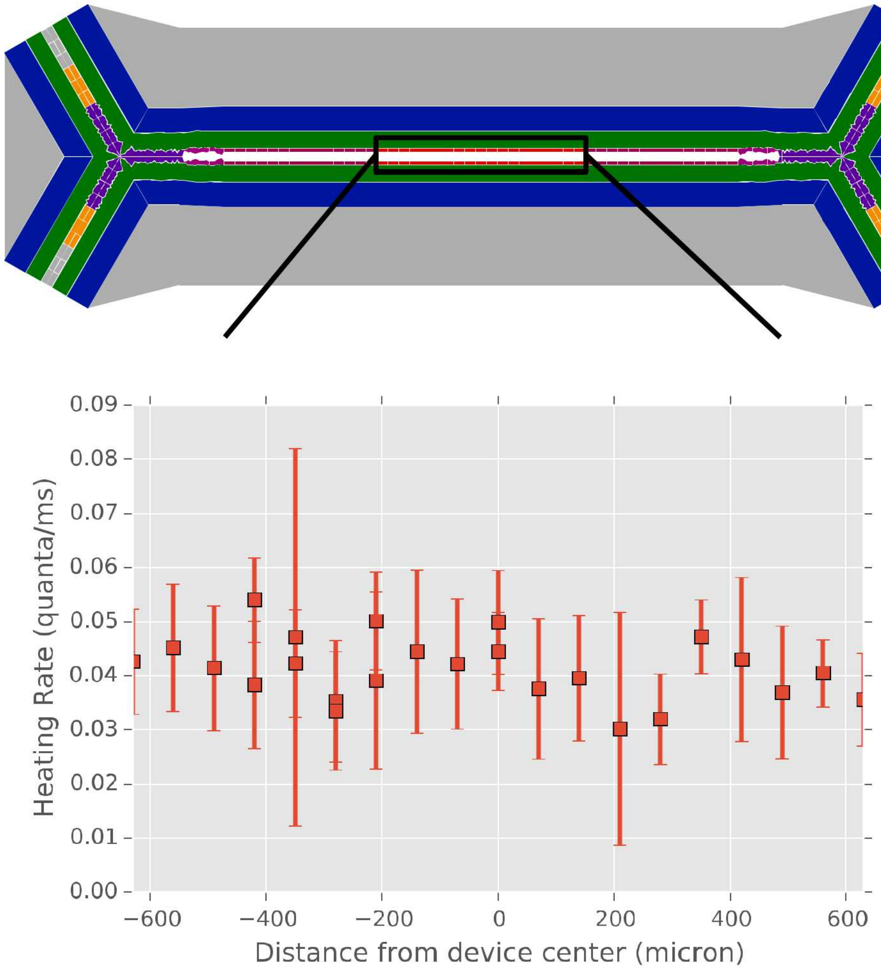

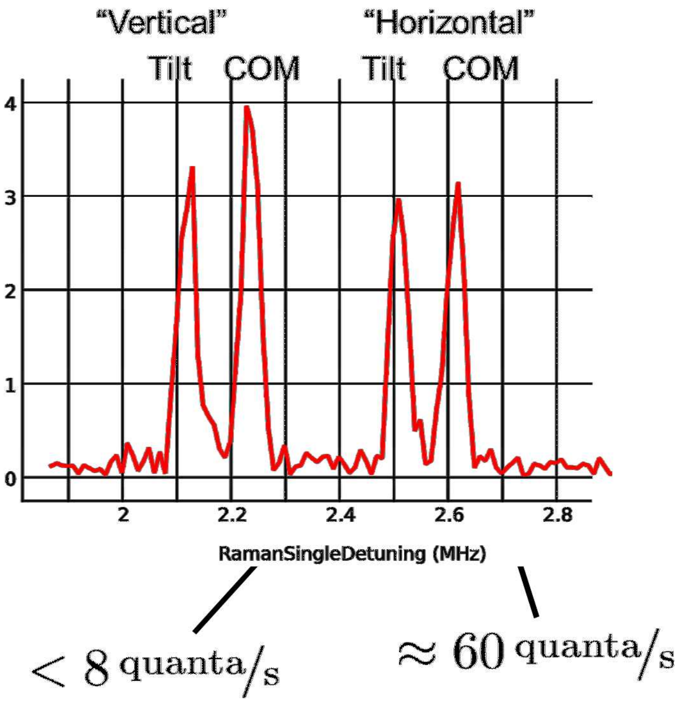

- Heating rate 40 q/s on average, $^{171}Yb^{+}$, Trap frequency 2.8 MHz, RF drive at 50 MHz
- Heating rate in HOA-2 is low and uniform along the length of the quantum section

Classical characterization

Background electric field

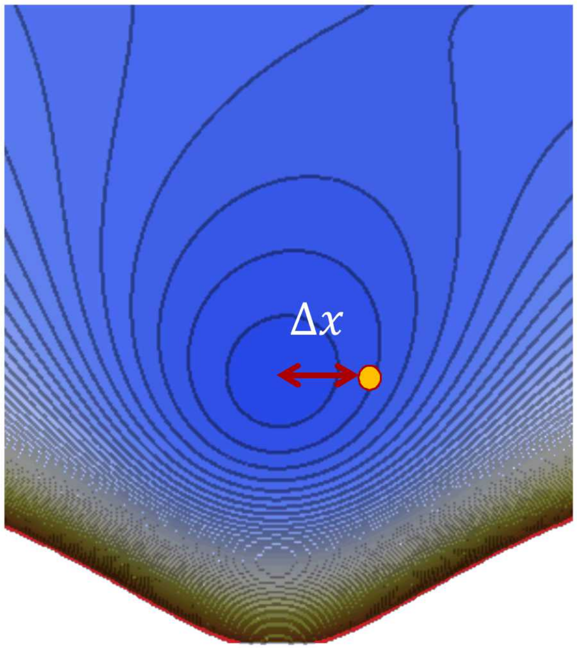

- Goal is to eliminate offset from RF null

$$x(t) = [A\cos(\omega t) + \Delta x](1 + \frac{q}{2}\cos(\Omega t))$$

- Measure transition strength of Raman beams applied at drive frequency (lateral direction)
- Tickle ion motion with chirped pulses at drive frequency, minimize fluorescence

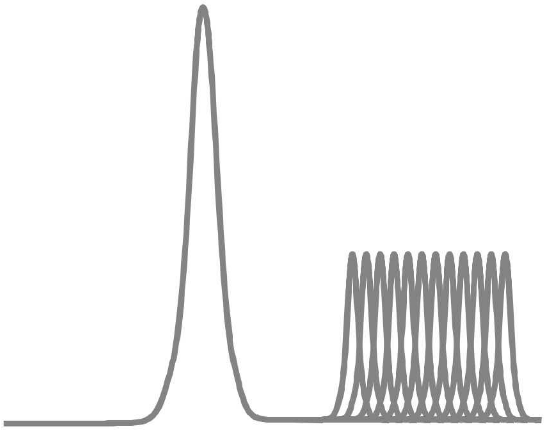

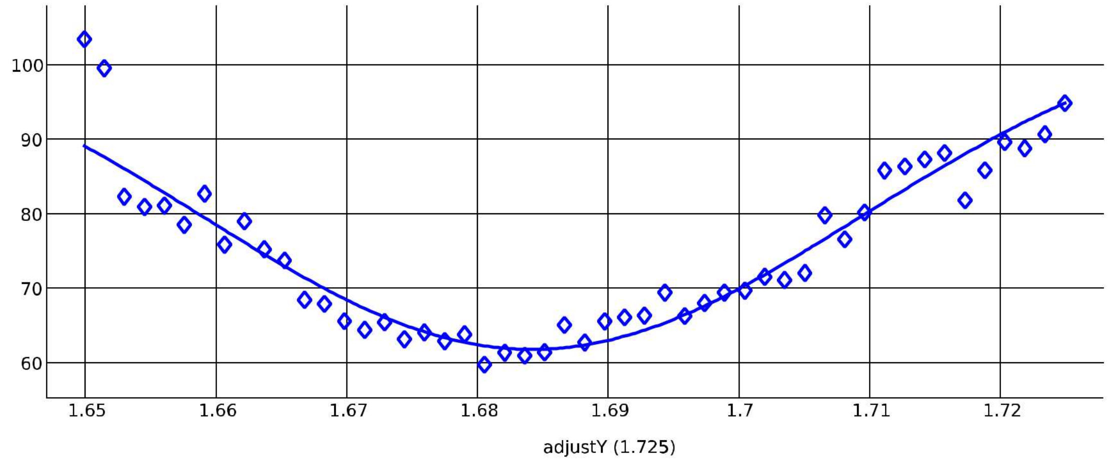

Background electric field

Linear trap

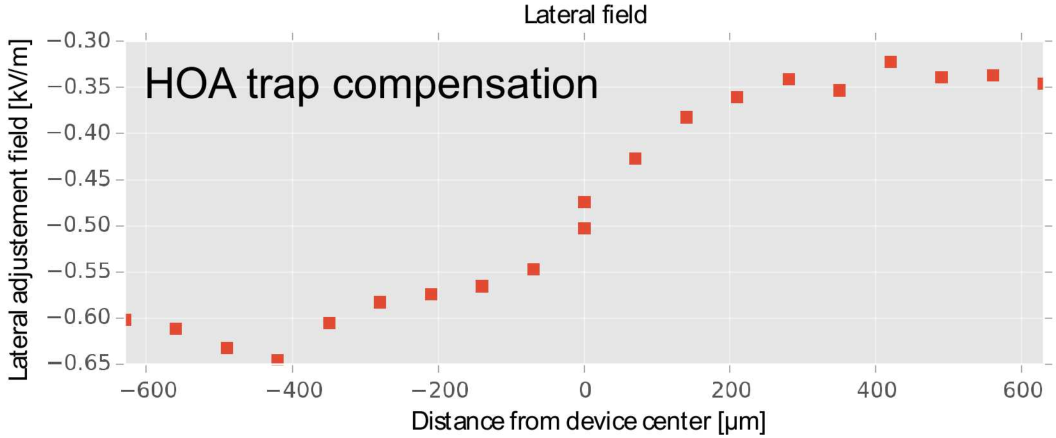

Ring trap

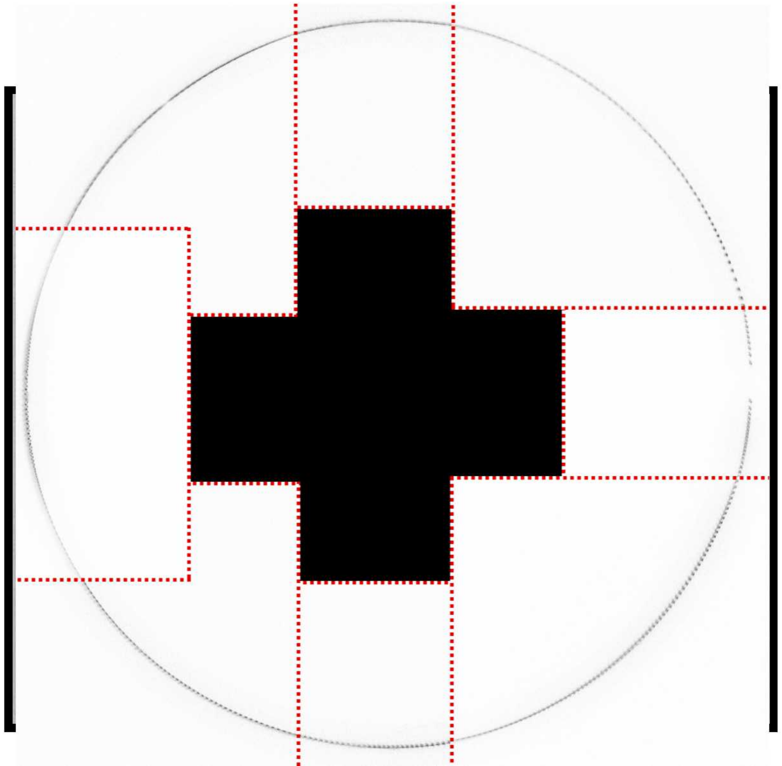

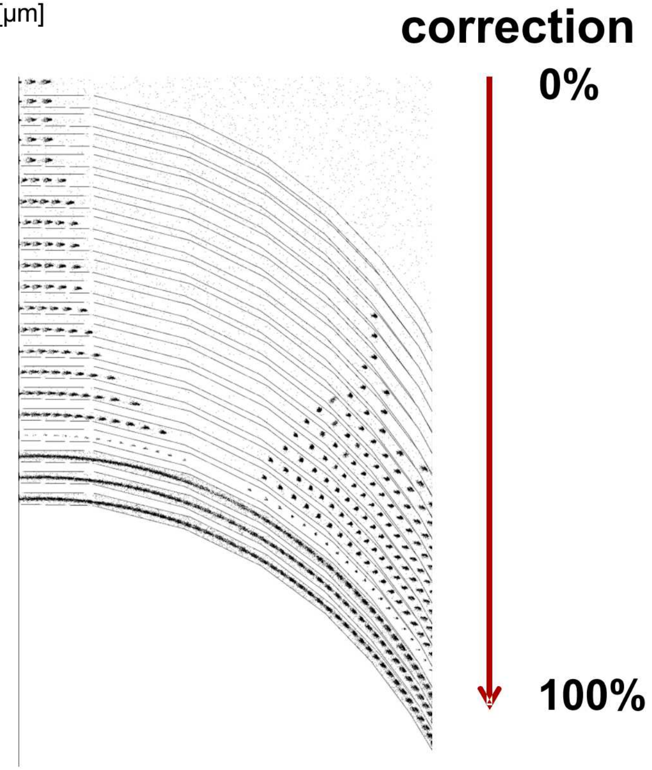

Classical characterization

Shuttling and swapping

- Co-wired junction and linear sections, transported ions around device
- Same voltage solution at junctions

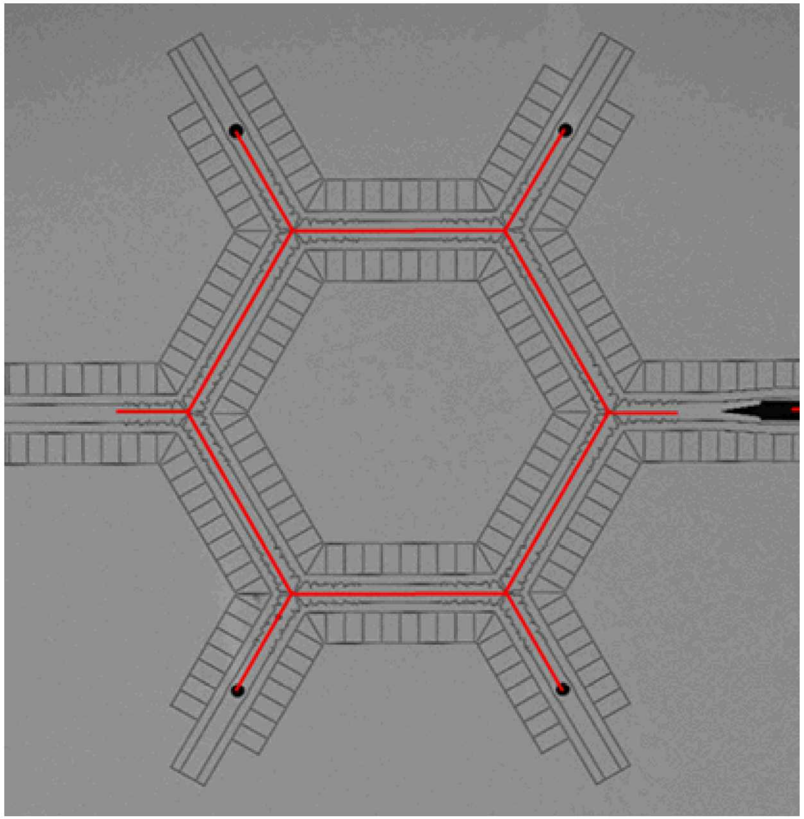

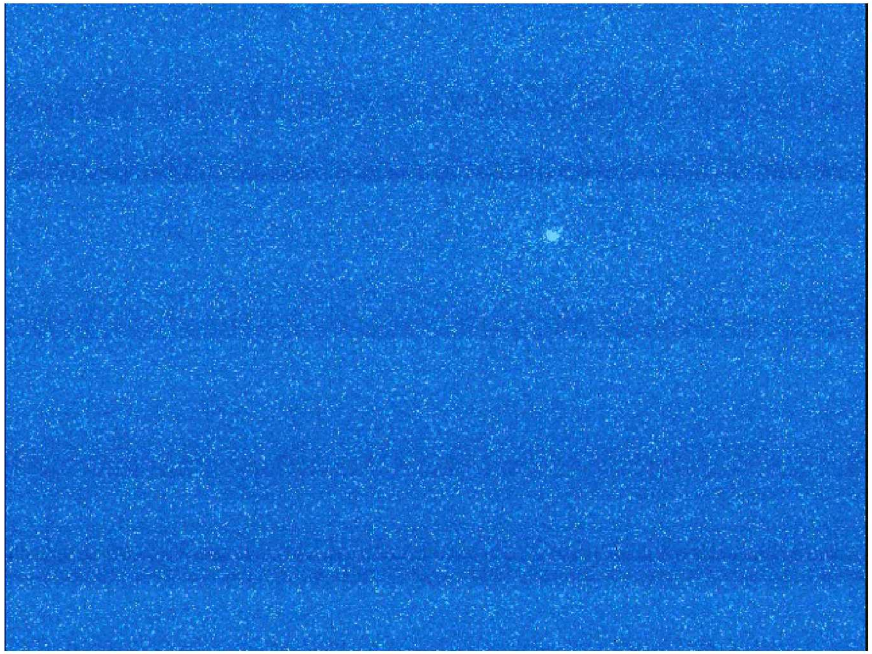

Classical characterization

Applications

Controlled rotation

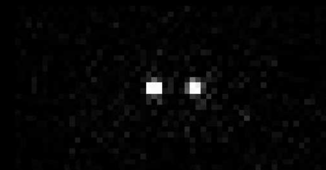

Combined rotation and translation

Separation and merging

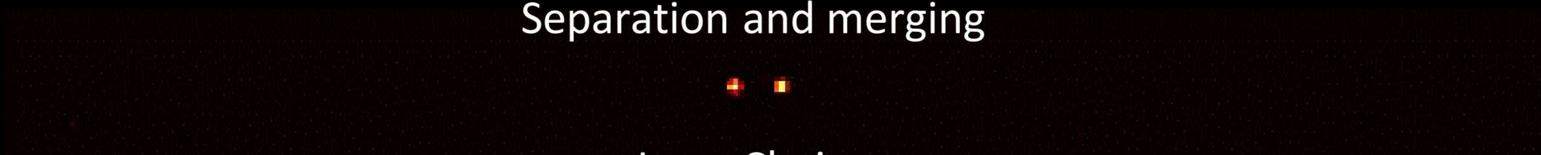

Long Chains

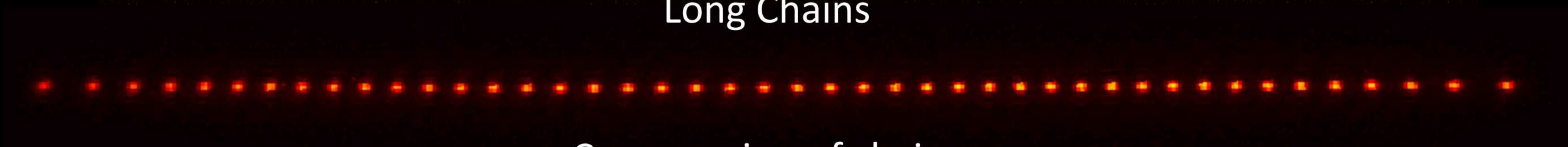

Compression of chains

3D Crystal Structures

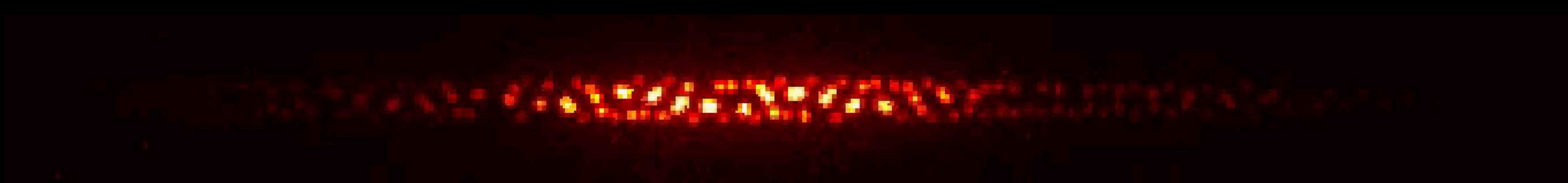

Outline

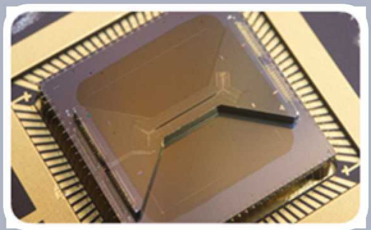

Ion trapology

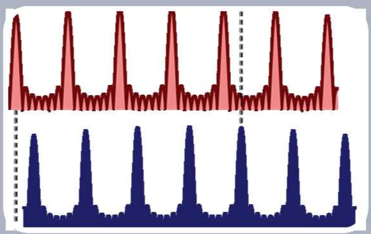

Classical characterization

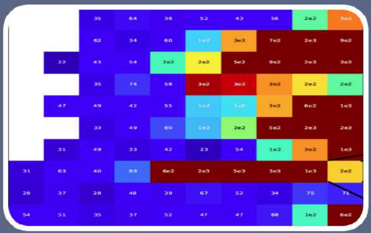

Quantum characterization

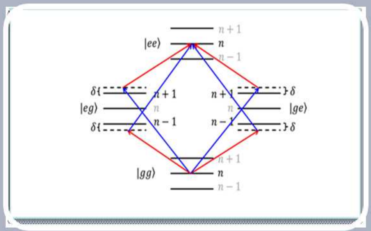

Specialized devices and Future directions

Single qubit gates

- Process infidelity ≈ diamond norm
  - This indicates that we have gotten rid of all systematic errors

Below the threshold for fault-tolerant error correction!

See P. Aliferis and A. W. Cross, Phys. Rev. Lett. 98, 220502 (2007)

Microwave Gates

Gate	Process Infidelity	1/2 ◊-Norm
G_I	$6.9(6) \times 10^{-5}$	$7.9(7) \times 10^{-5}$
G_X	$6.1(7) \times 10^{-5}$	$7.0(15) \times 10^{-5}$
G_Y	$7.2(7) \times 10^{-5}$	$8.1(15) \times 10^{-5}$

Laser Gates

co-propagating

Gate	Process Infidelity	1/2 ◊-Norm
G_I	$1.17(7) \times 10^{-4}$	$5.3(2) \times 10^{-4}$
G_X	$5.0(7) \times 10^{-5}$	$3(6) \times 10^{-4}$
G_Y	$6.9(6) \times 10^{-5}$	$4(9) \times 10^{-4}$

counter-propagating

Gate	Process Infidelity	1/2 ◊-Norm
G_I	$11.1(6) \times 10^{-4}$	$22.8(1) \times 10^{-4}$
G_X	$4.0(4) \times 10^{-4}$	$13.2(6) \times 10^{-4}$
G_Y	$4.1(4) \times 10^{-4}$	$8.4(8) \times 10^{-4}$

- Co-propagating gates have infidelity comparable to microwave gates, but diamond norm indicates some residual control errors

- Counter-propagating gates are noticeably worse, but are necessary for two-qubit gates
- Lower fidelity presumably results from anomalous heating and optical phase sensitivity

Outline

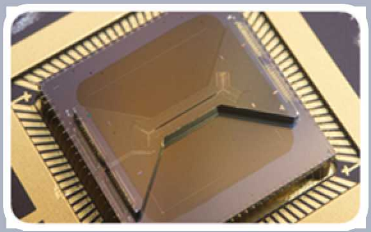

Ion trapology

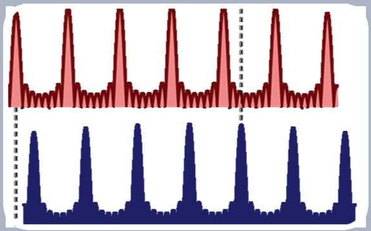

Classical characterization

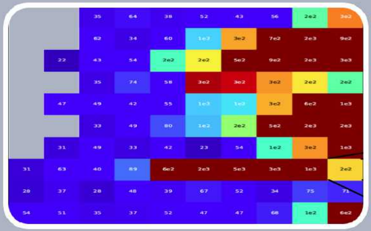

Quantum characterization

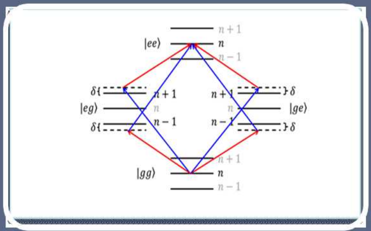

Specialized devices and Future directions

Microwave trap

Benefits:

- Microwave radiation is easier to control and cheaper to implement than lasers
- Low power for Rabi oscillations (330 ns for -2 dB at device)
- Near field allows to generate microwave gradient fields

Challenges:

- Microwave delivery (-17 dB loss chamber to dev)
- Dissipation, heating, thermal management

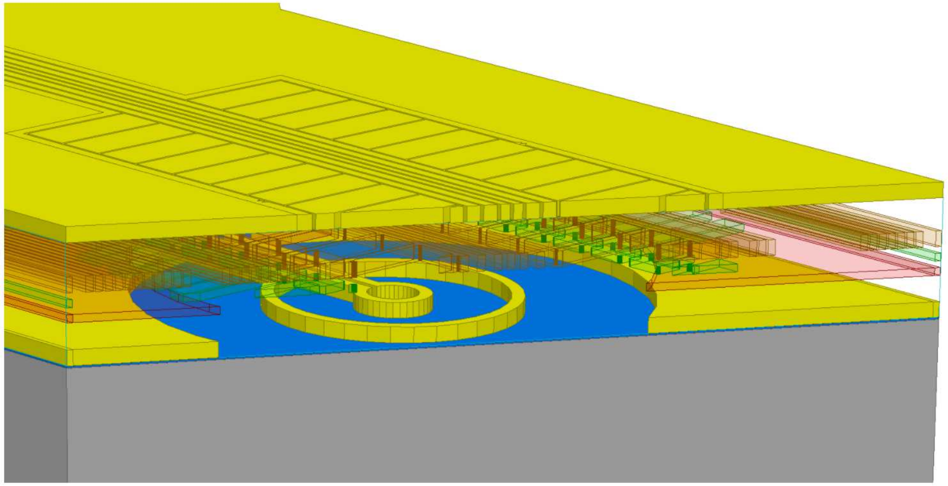

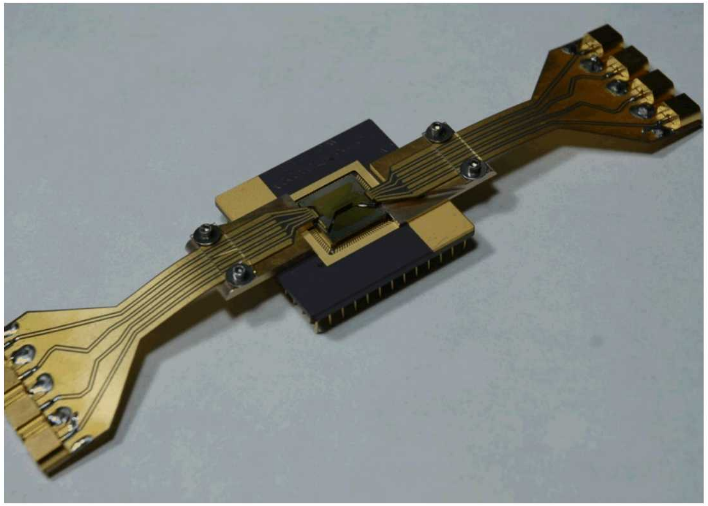

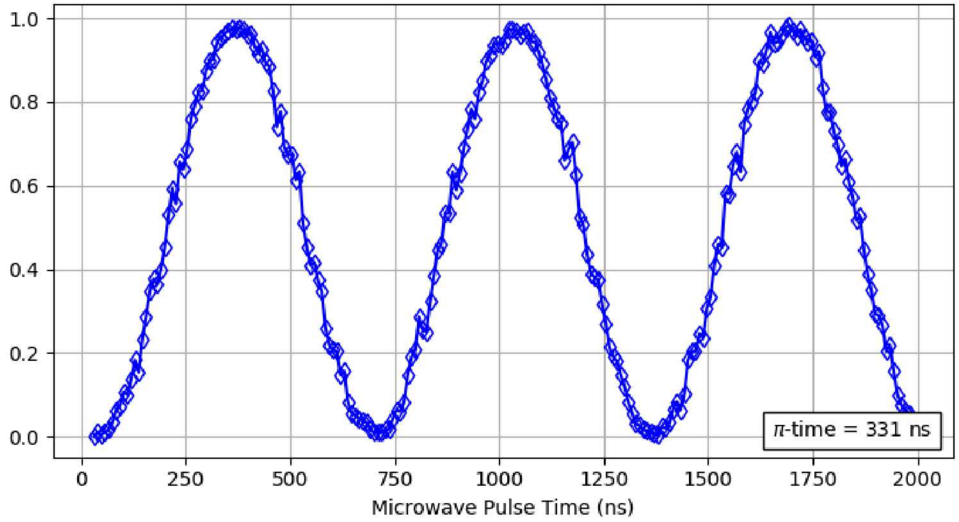

TICTOC optical clock

An atomic-photonic integrated clock to achieve

$\sigma_y < 1 \times 10^{-14}/\tau^{1/2}$ for

$1\ \mathbf{s} < \tau < 100{,}000\ \mathbf{s}$

in less than ½ liter

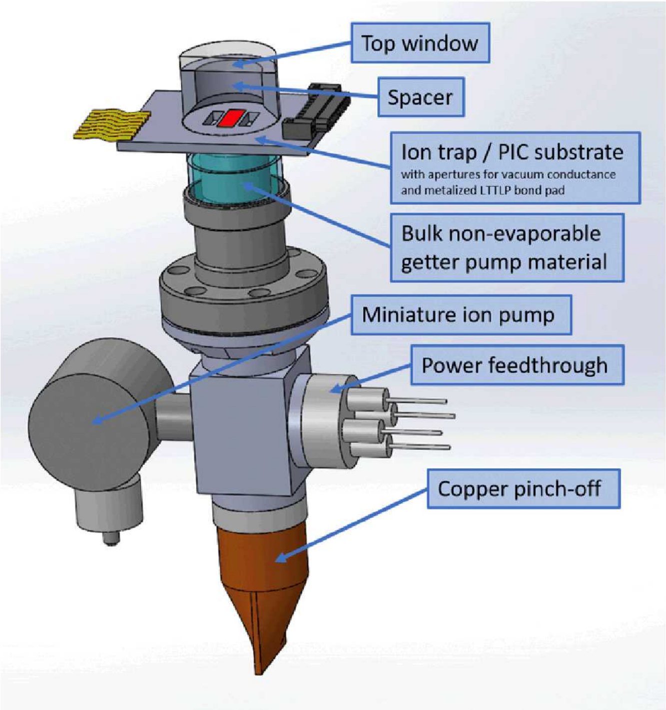

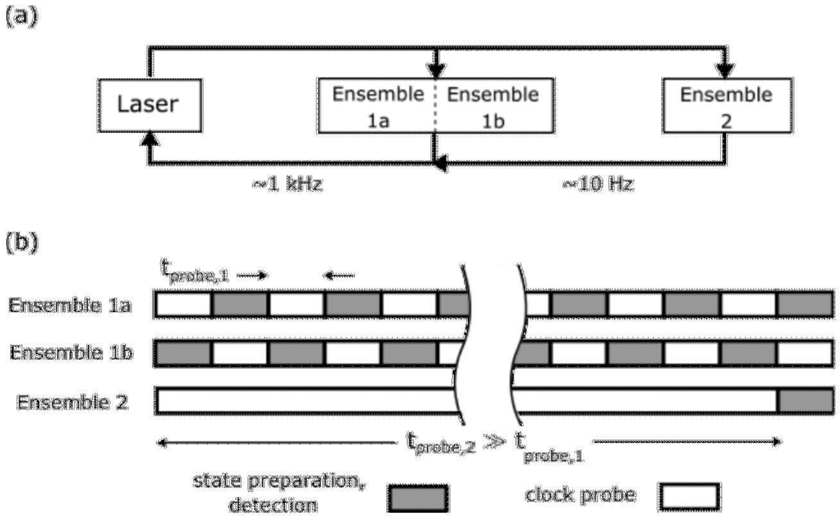

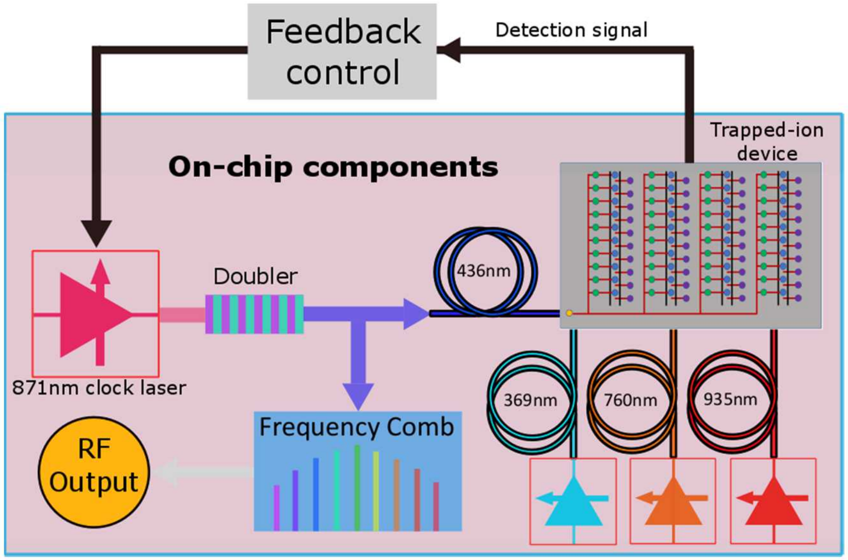

QSCOUT (QS Open User Testbed)

Trapped Ions: fully connected

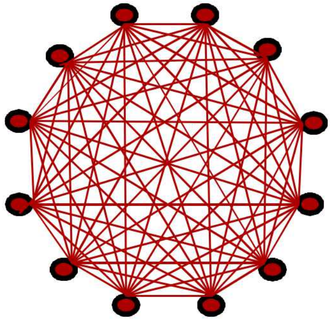

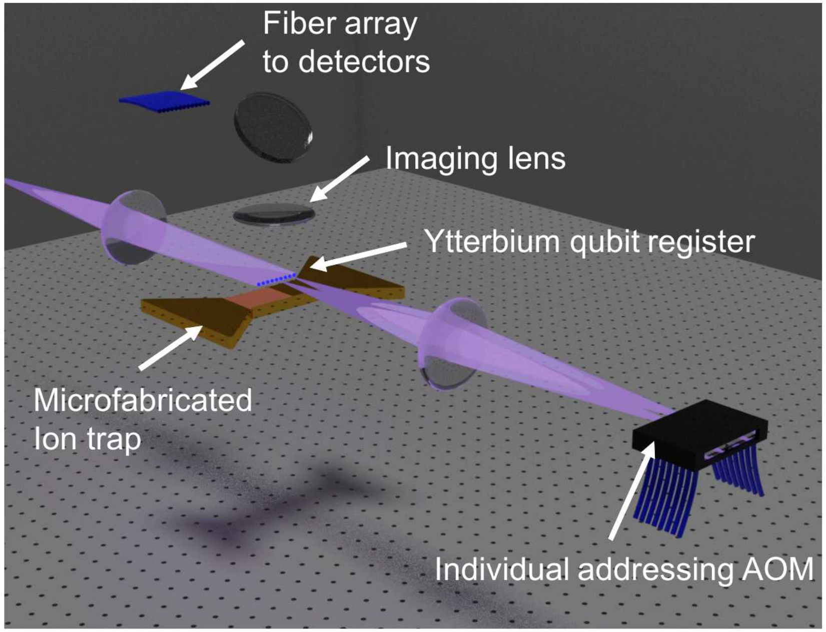

- Single chain of 5 – 15 ytterbium qubits
- Stored in Sandia surface trap
- Individual addressing with 355nm Raman beams
- Full connectivity using radial vibrational modes
- Individual qubit detection via fiber array
- Addressing and detection supports up to 32 qubits

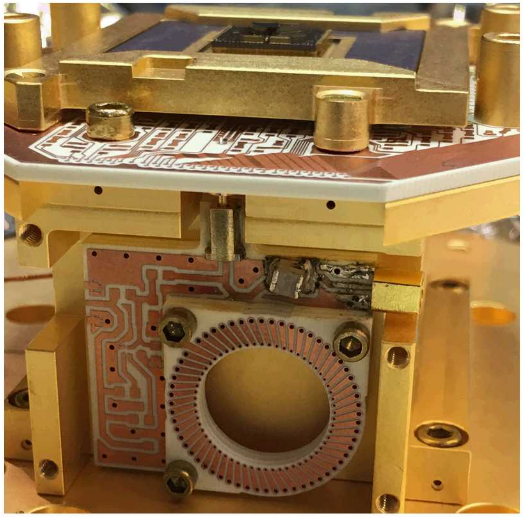

Acknowledgments

U.S. DEPARTMENT OF ENERGY

LDRD LABORATORY DIRECTED RESEARCH & DEVELOPMENT

DARPA

CQuIC

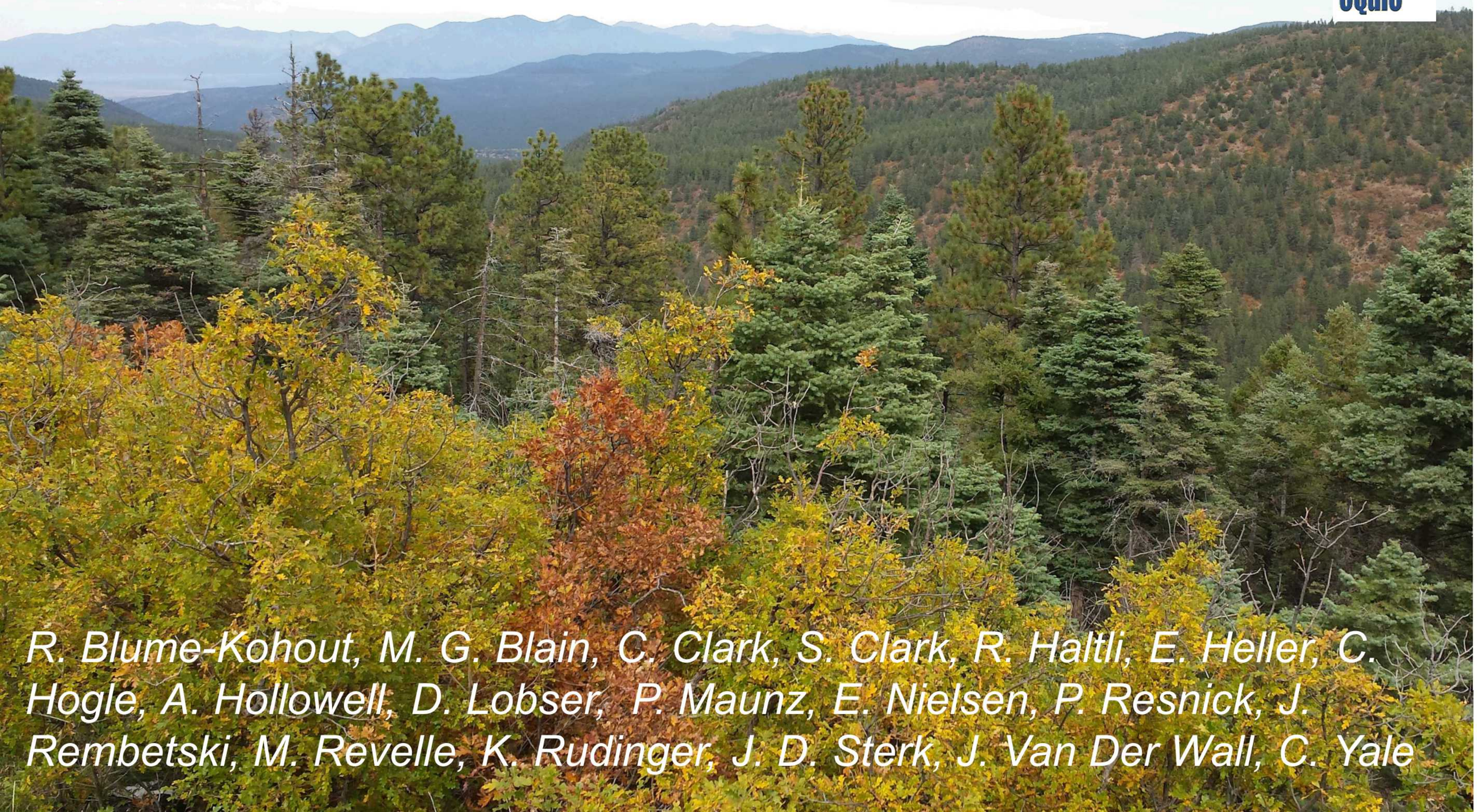

R. Blume-Kohout, M. G. Blain, C. Clark, S. Clark, R. Haltli, E. Heller, C. Hogle, A. Hollowell, D. Lobser, P. Maunz, E. Nielsen, P. Resnick, J. Rembetski, M. Revelle, K. Rudinger, J. D. Sterk, J. Van Der Wall, C. Yale

Shuttling and swapping

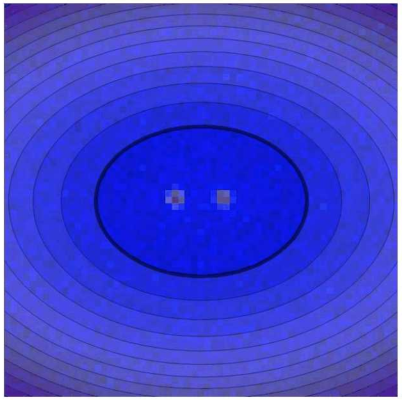

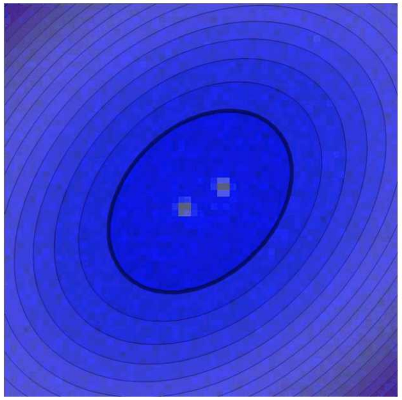

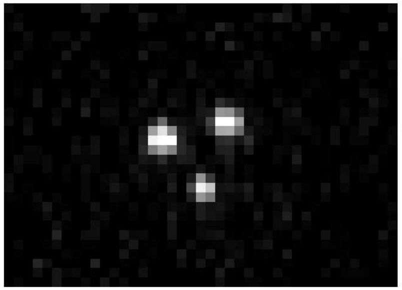

- Tag one ion with BB1 composite pulse
- Measure states on separate PMT's after rotation
  - In addition to declining success probability, fluorescence drops due to motional heating
  - Success probability drops for times <18.6 us

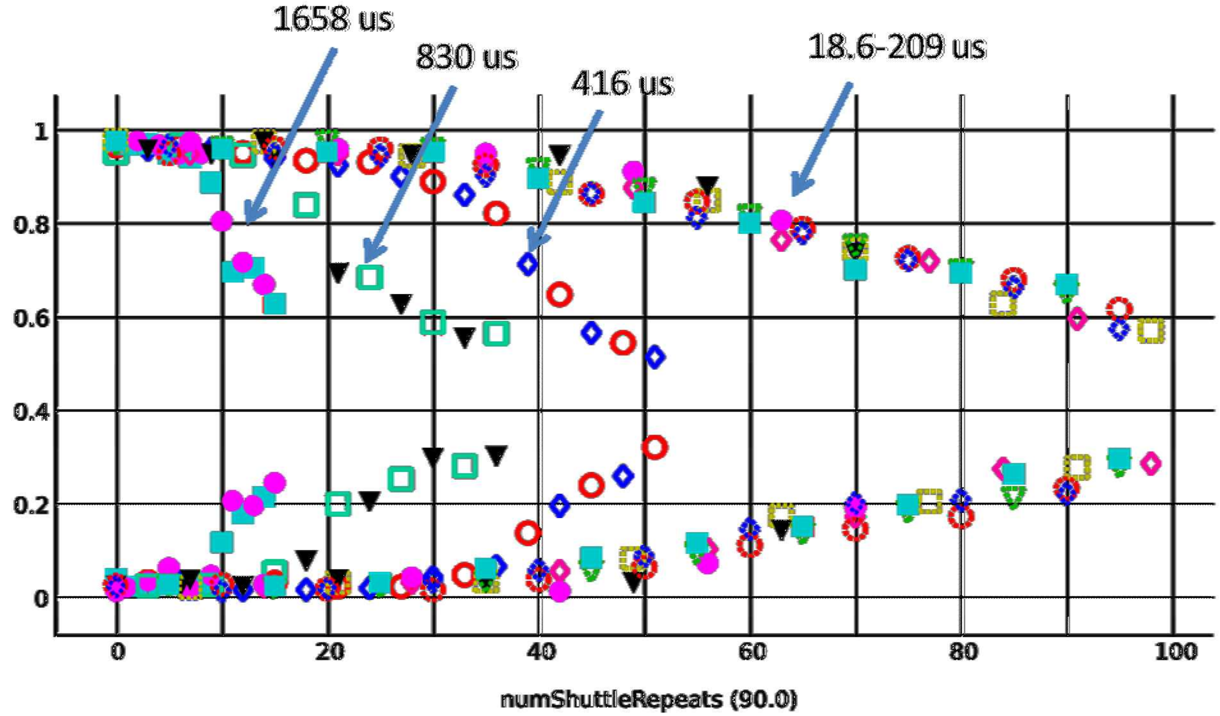

Ytterbium qubit

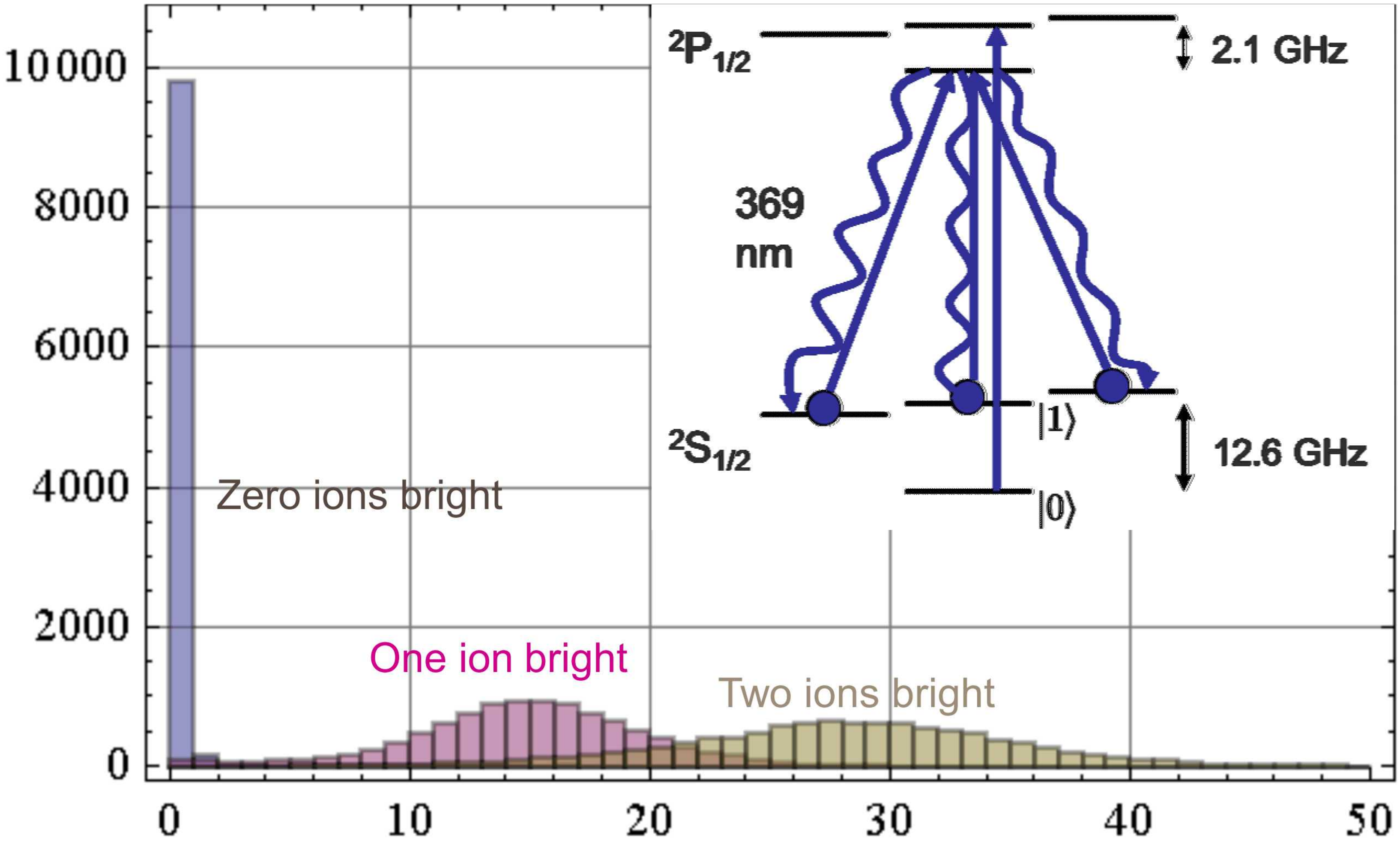

S. Olmschenk *et al.*, PRA **76**, 052314 (2007)

Ytterbium qubit

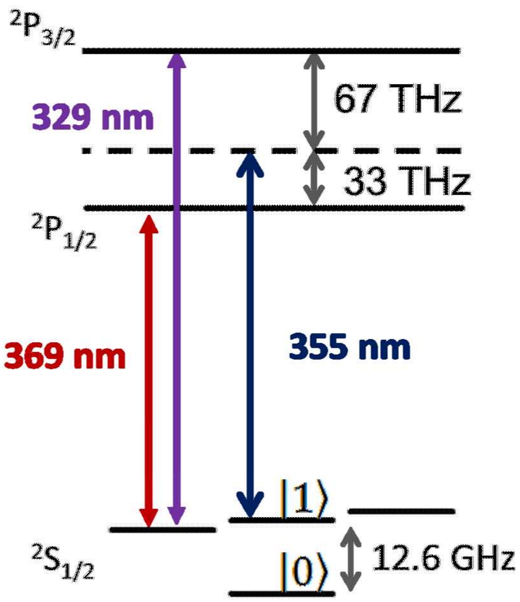

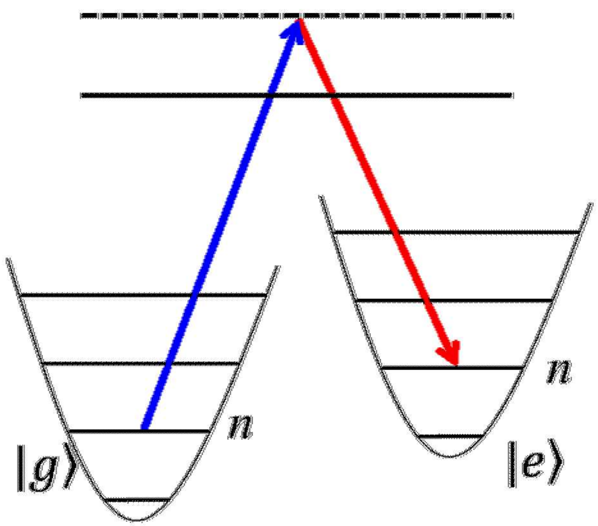

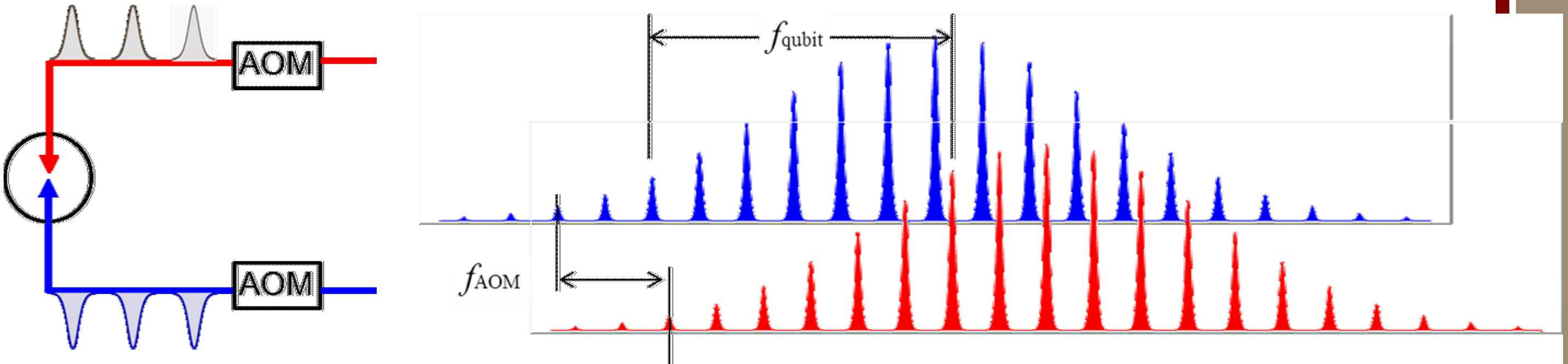

Gate Set Tomography (GST)

- No calibration required
- Detailed debug information
- Efficiently measures performance characterizing fault-tolerance (diamond norm)
- Amplifies errors
- Detects non-Markovian noise
- Robin Blume-Kohout, SNL

Desired "target" gates:

G_i	Idle (Identity)
G_x	$\pi/2$ rotation about x-axis
G_y	$\pi/2$ rotation about y-axis

Fiducials:

$\{\}$

Gx

Gy

$Gx \cdot Gx$

$Gx \cdot Gx \cdot Gx$

$Gy \cdot Gy \cdot Gy$

Germs:

Gx

Gy

Gi

$Gx \cdot Gy$

$Gx \cdot Gy \cdot Gi$

$Gx \cdot Gi \cdot Gy$

$Gx \cdot Gi \cdot Gi$

$Gy \cdot Gi \cdot Gi$

$Gx \cdot Gx \cdot Gi \cdot Gy$

$Gx \cdot Gy \cdot Gy \cdot Gi$

$Gx \cdot Gx \cdot Gy \cdot Gx \cdot Gy \cdot Gy$

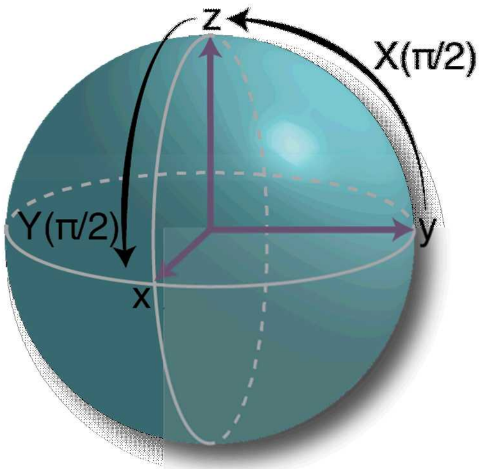

Single qubit BB1 compensated microwave gates on $^{171}Yb^{+}$

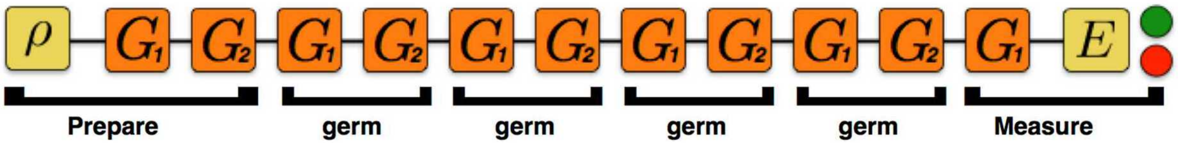

Microwave gates

Raw data poor gates

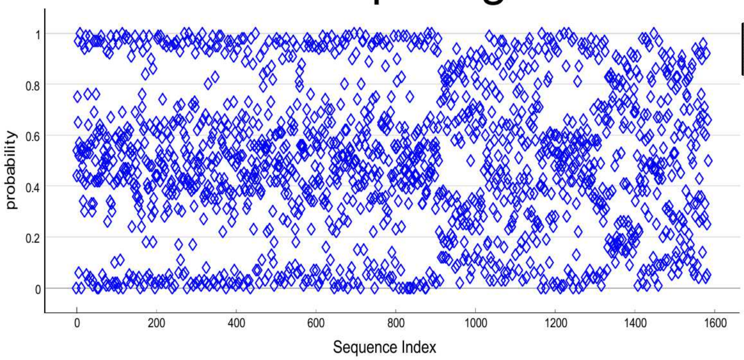

Raw data good gates

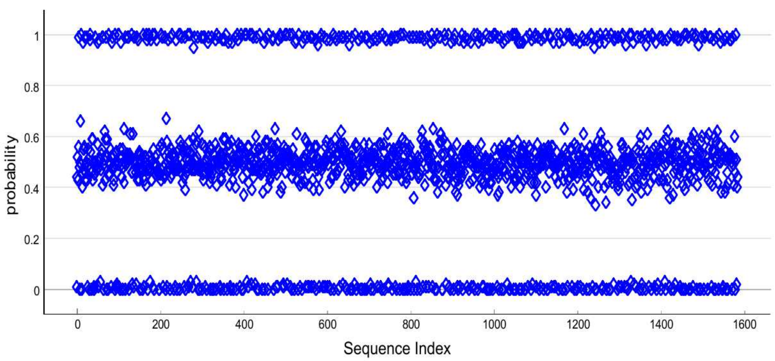

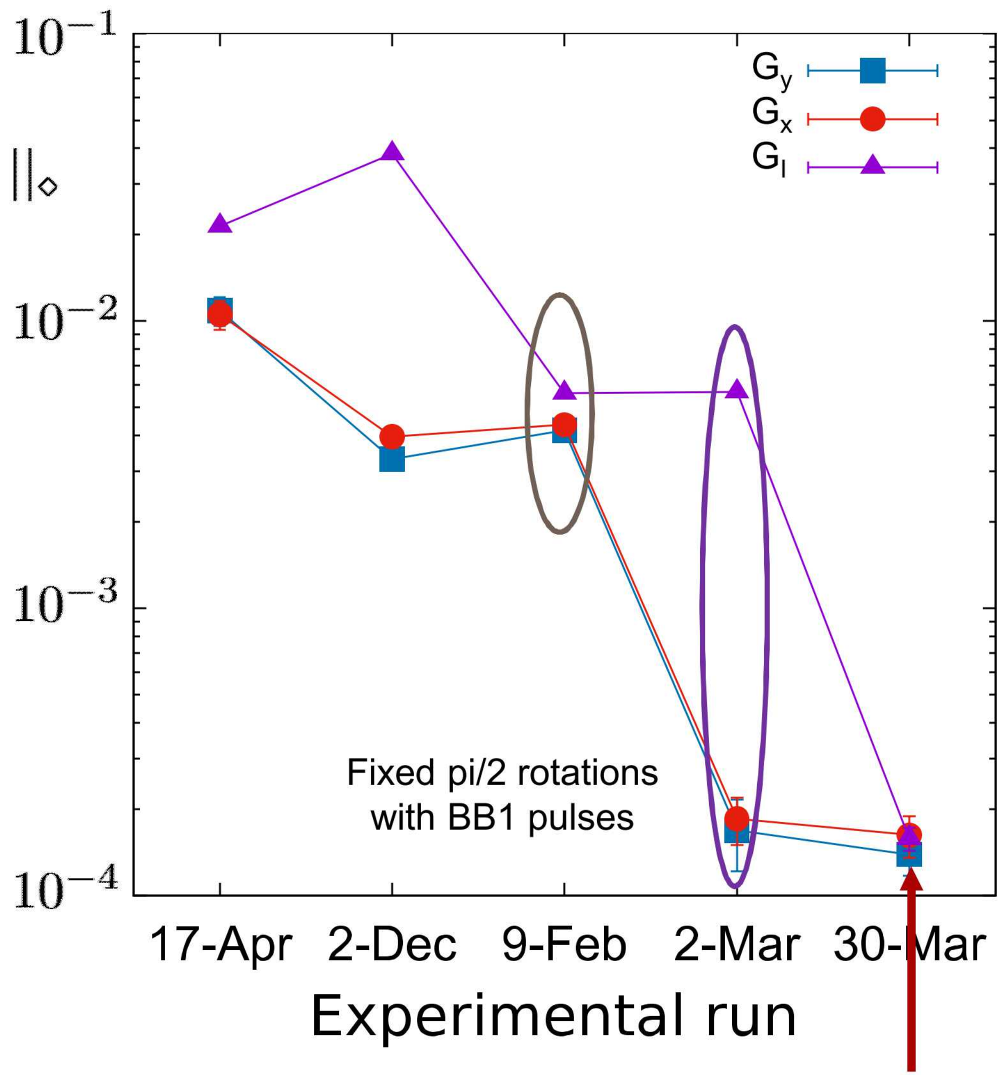

Fixed drift and context dependency

Error mitigation

Compensated Pulses

- BB1-type dynamical-decoupling pulses used
- Corrects pulse-length errors

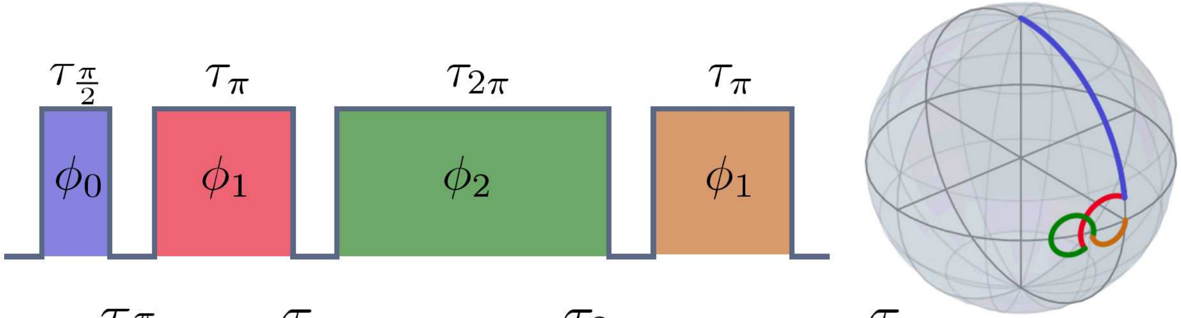

"Gapless" Pulses

- Phase changed discontinuously on DDS
- Avoids finite turn-on time effects
- Removes errors caused by asynchronous pulse arrival
- Allows for continuous power stabilization

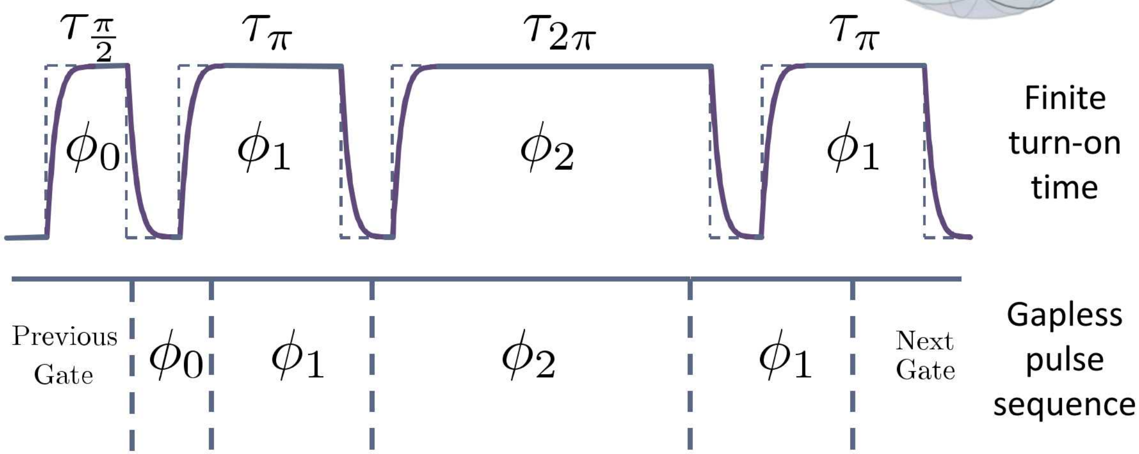

Drift Control

(Drive Frequency)

- Single-shot calibrations increase or decrease a control parameter by a negligible value
- Small corrections either average out or slowly accumulate

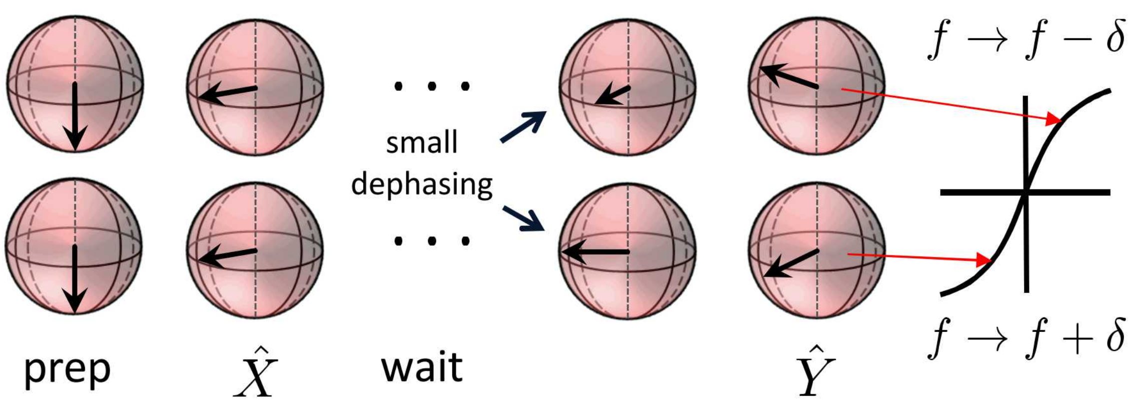

Two qubit gates

- Bichromatic entangling "Mølmer-Sørensen" gate
- Gate time and detuning from motional sidebands is set so that population in motionally (de-)excited states is zero corresponding to a closed loop in phase space
- Does not require ground state cooling
- Requires a number of extra calibrations
    - Rabi frequencies of red/blue detuned transitions matched
    - Ions need to be evenly illuminated
    - Phase of beat note needs to be calibrated and stable

$$|00\rangle \rightarrow |00\rangle + |11\rangle$$

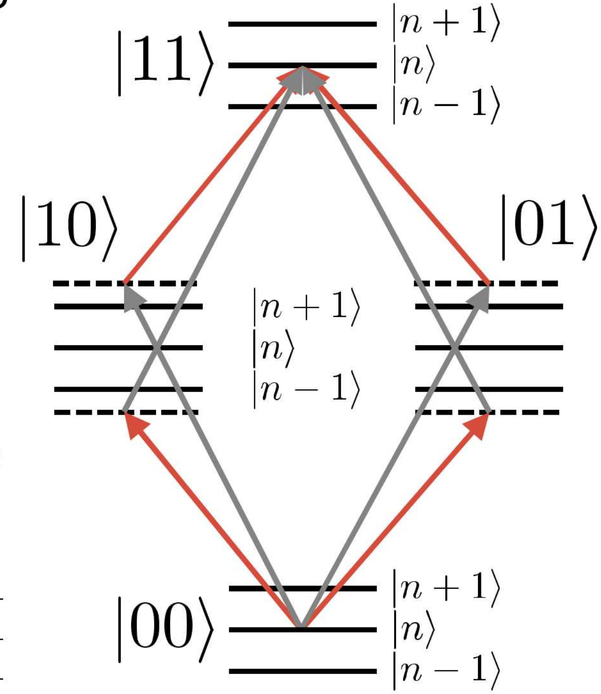

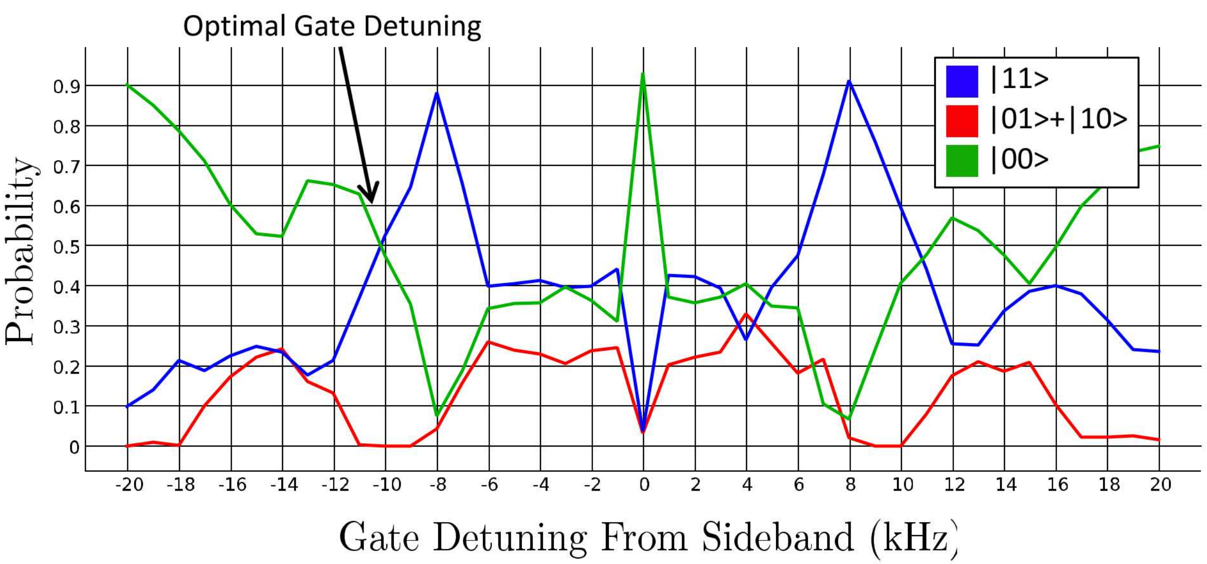

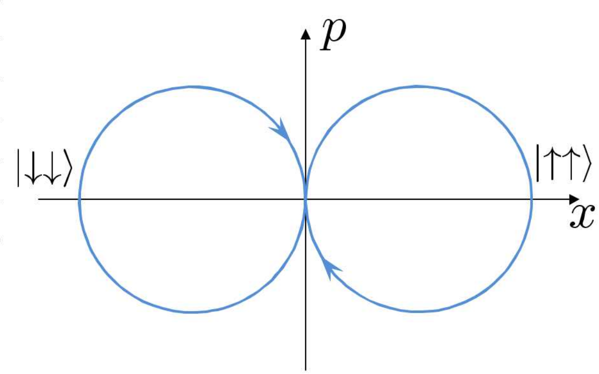

Two qubit gates

Typical Approach: <u>Entangled State Fidelity</u>

- Entangled state fidelity determined by

$$\mathcal{F} = \frac{1}{2}\left(P(|00\rangle) + P(|11\rangle)\right) + \frac{1}{4}c$$

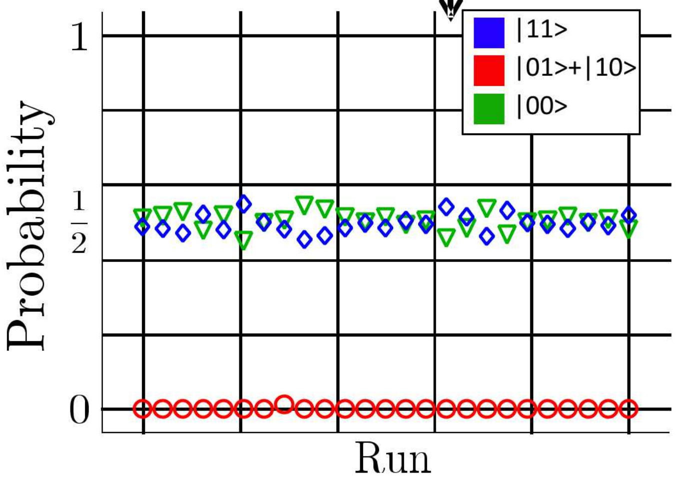

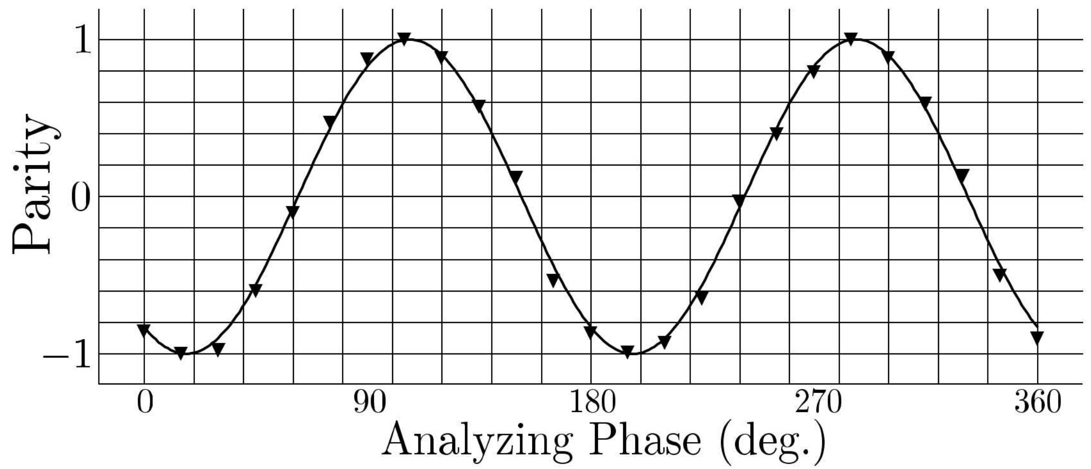

- Repeated application of gate
- Measure average population of entangled state

- Apply gate followed by analyzing pulse of varying phase
- Measure the resulting contrast

Two qubit gates

Typical Approach: <u>Entangled State Fidelity</u>

$$\mathcal{F} = \frac{1}{2}\left(P(|00\rangle) + P(|11\rangle)\right) + \frac{1}{4}c \approx 0.995$$

<u>Two-Qubit GST</u>

- Provides a true *process* fidelity
- Requires an extremely stable gate to take long GST measurements without constant recalibration

- Currently limited to the symmetric subspace

Gate	Process infidelity	$\frac{1}{2}$ Diamond norm
G_I	$1.6 \times 10^{-3} \pm 1.6 \times 10^{-3}$	$28 \times 10^{-3} \pm 7 \times 10^{-3}$
G_{XX}	$0.4 \times 10^{-3} \pm 1.0 \times 10^{-3}$	$27 \times 10^{-3} \pm 5 \times 10^{-3}$
G_{YY}	$0.1 \times 10^{-3} \pm 0.9 \times 10^{-3}$	$26 \times 10^{-3} \pm 4 \times 10^{-3}$
G_{MS}	$4.2 \times 10^{-3} \pm 0.6 \times 10^{-3}$	$38 \times 10^{-3} \pm 5 \times 10^{-3}$

95% confidence intervals

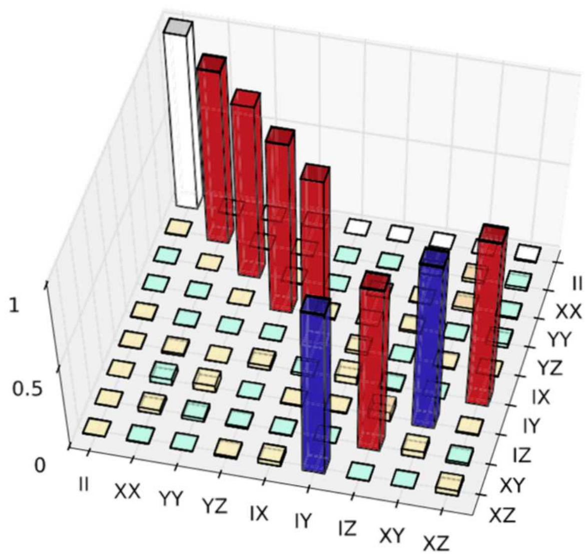

$$F_{MS} = 0.9958(6)$$

$$\frac{1}{2}||G_{MS}||_\diamond = 0.08(1)$$

- Much more rigorous characterization
- Gate is stable for several hours

Specialized devices & Future directions
EPICS trap

- Integrated Superconducting Nanowire Single-Photon Detector (SNSPD) detector and reflective backplane
  - Detector developed by JPL/NIST
- SNSPD provides higher photon detection (>80% vs <30%)
- Cavity-QED provides higher photon collection efficiency
- Strong coupling regime enables qubit measurement via fast cavity transmission
- Extra rf electrodes enable alignment of rf node with cavity modes

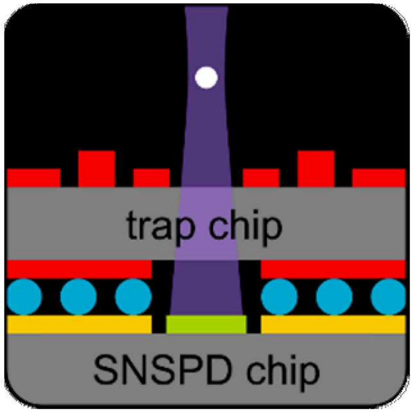

Ion Trap Fabrication (Duke/SNL)

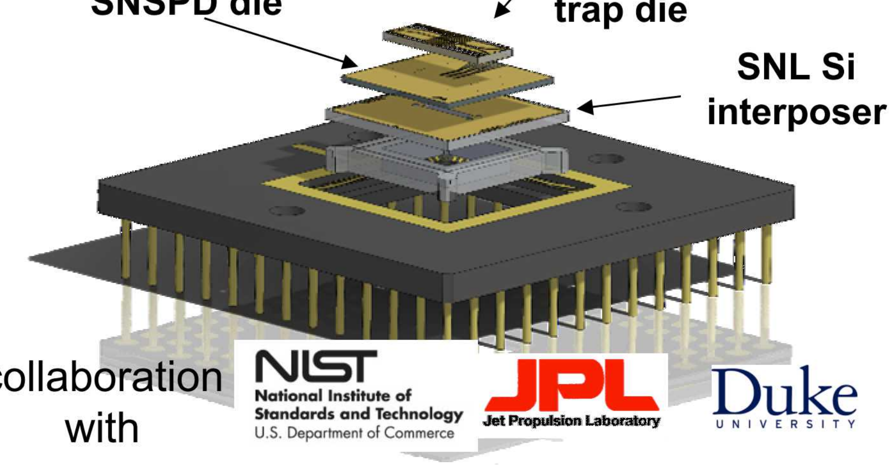

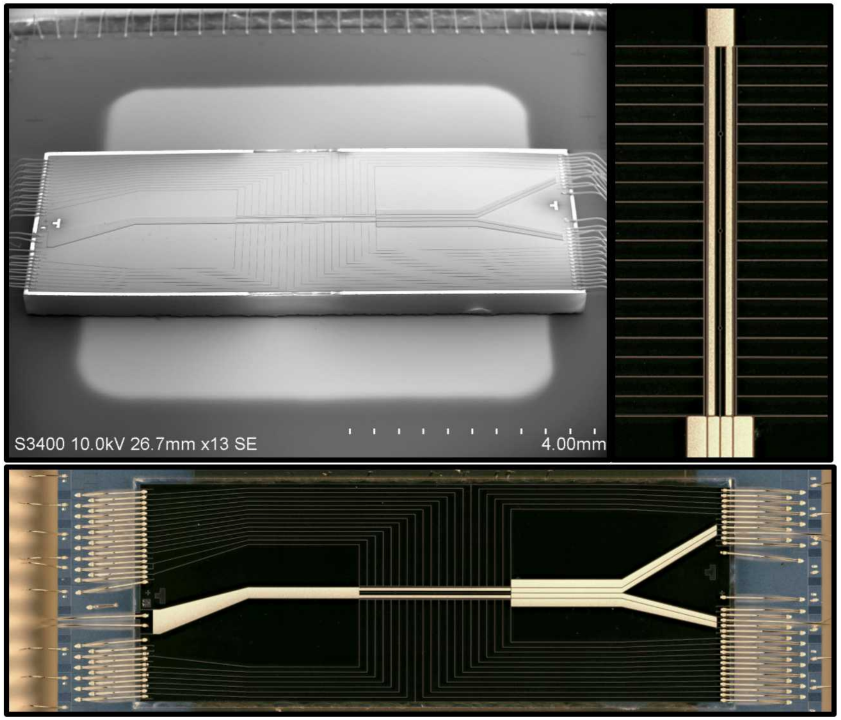

collaboration with

NIST National Institute of Standards and Technology U.S. Department of Commerce

JPL Jet Propulsion Laboratory

Duke UNIVERSITY

Trap features

Manufacturability, uniformity

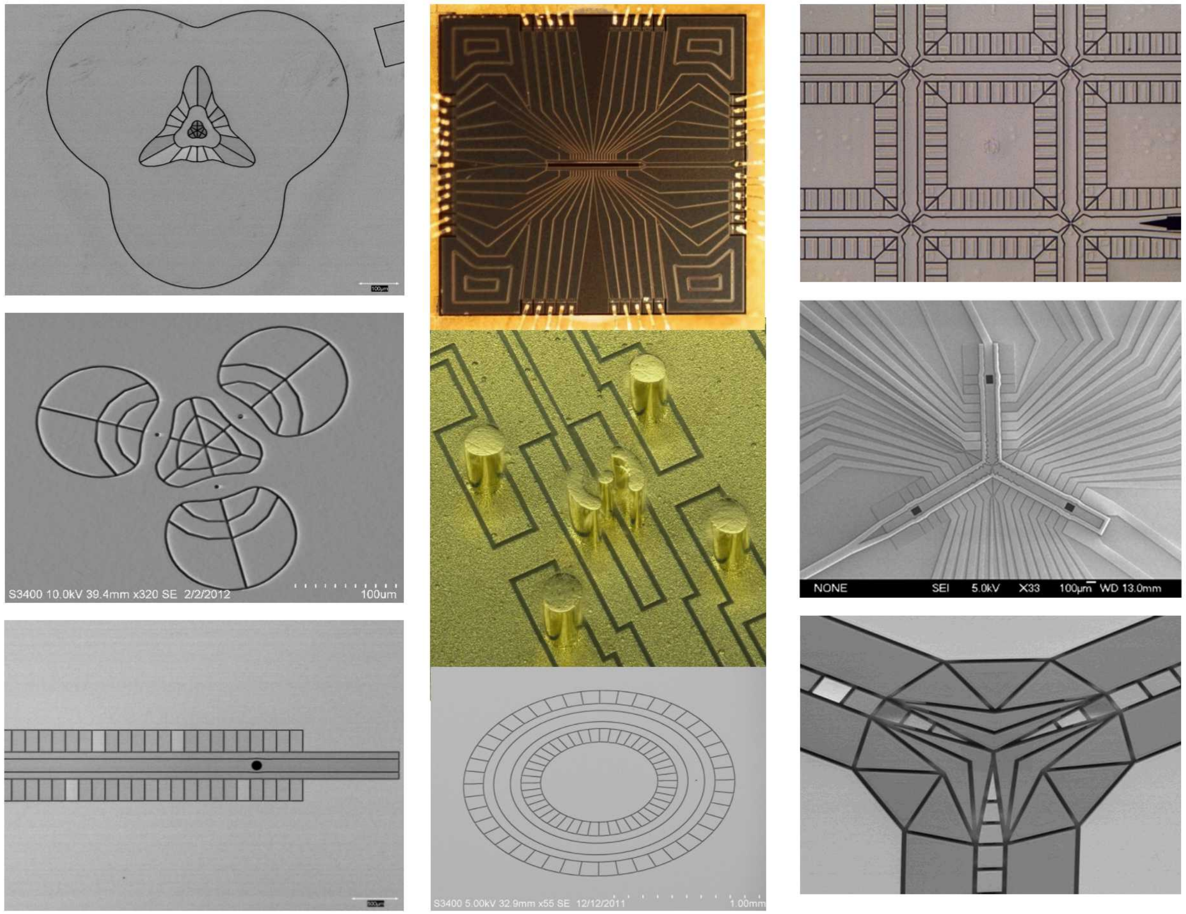

- 12 institutions, 5 countries
- >100 devices delivered
- Quantum computing
- Quantum simulations
- Quantum communication
- Surface science
- Metrology

Shuttling and swapping

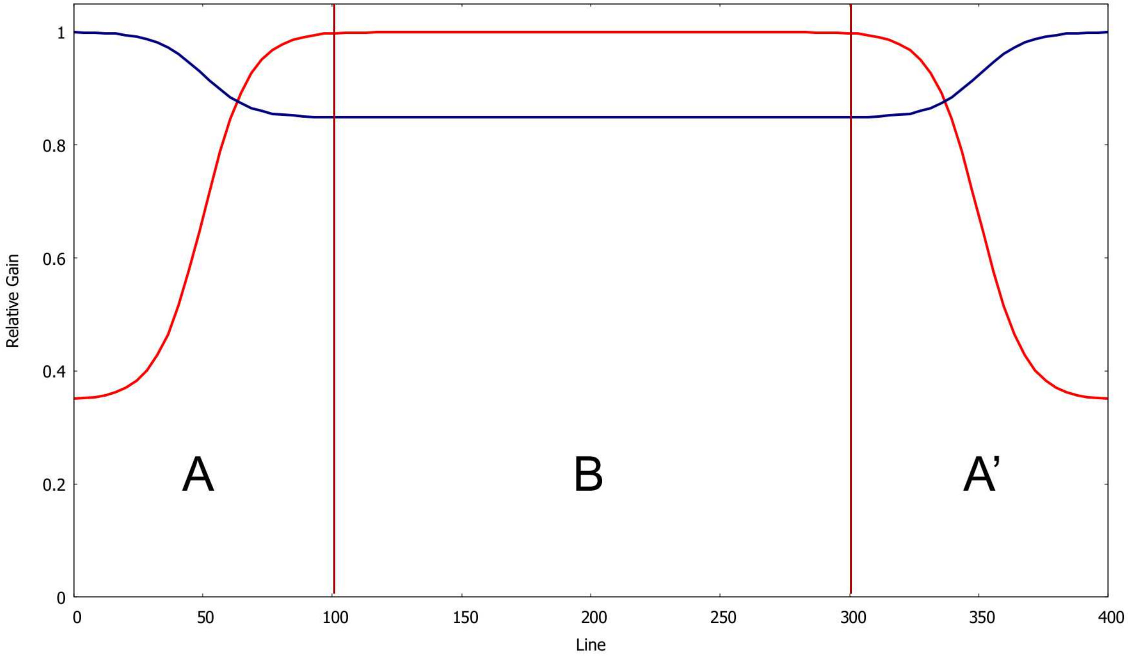

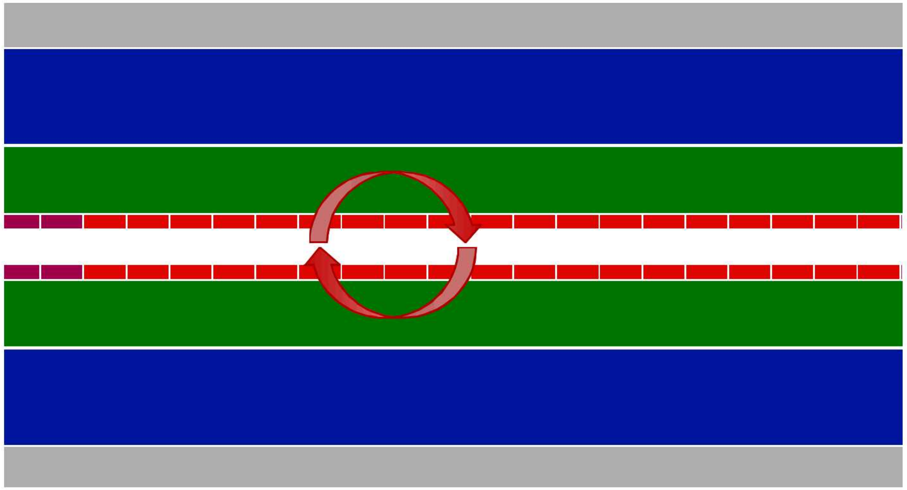

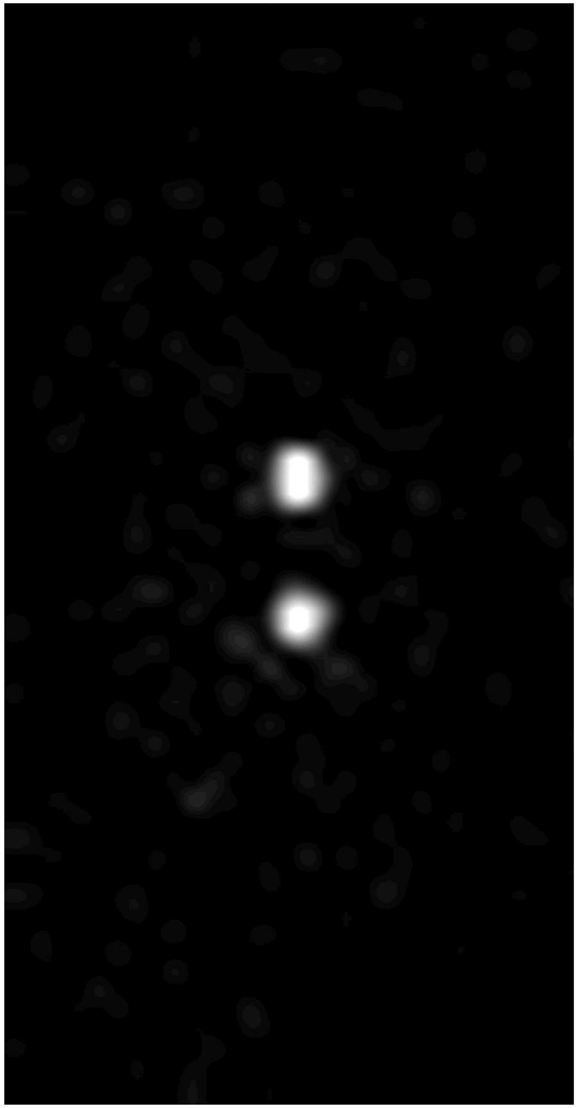

Microwave gates

Raw data poor gates

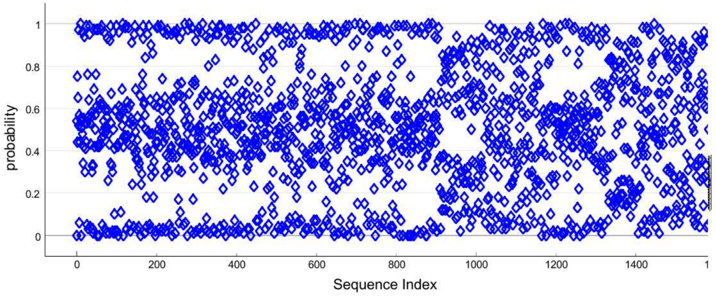

Gate	Rotn. axis	Angle
G_I	0.5252 -0.009 0.8506 -0.0244	0.001699π
G_X	-3×10^{-6} -1 -3×10^{-5} -0.009	0.501308π
G_Y	-0.2474 0.0001 0.9689 -0.0001	0.501366π

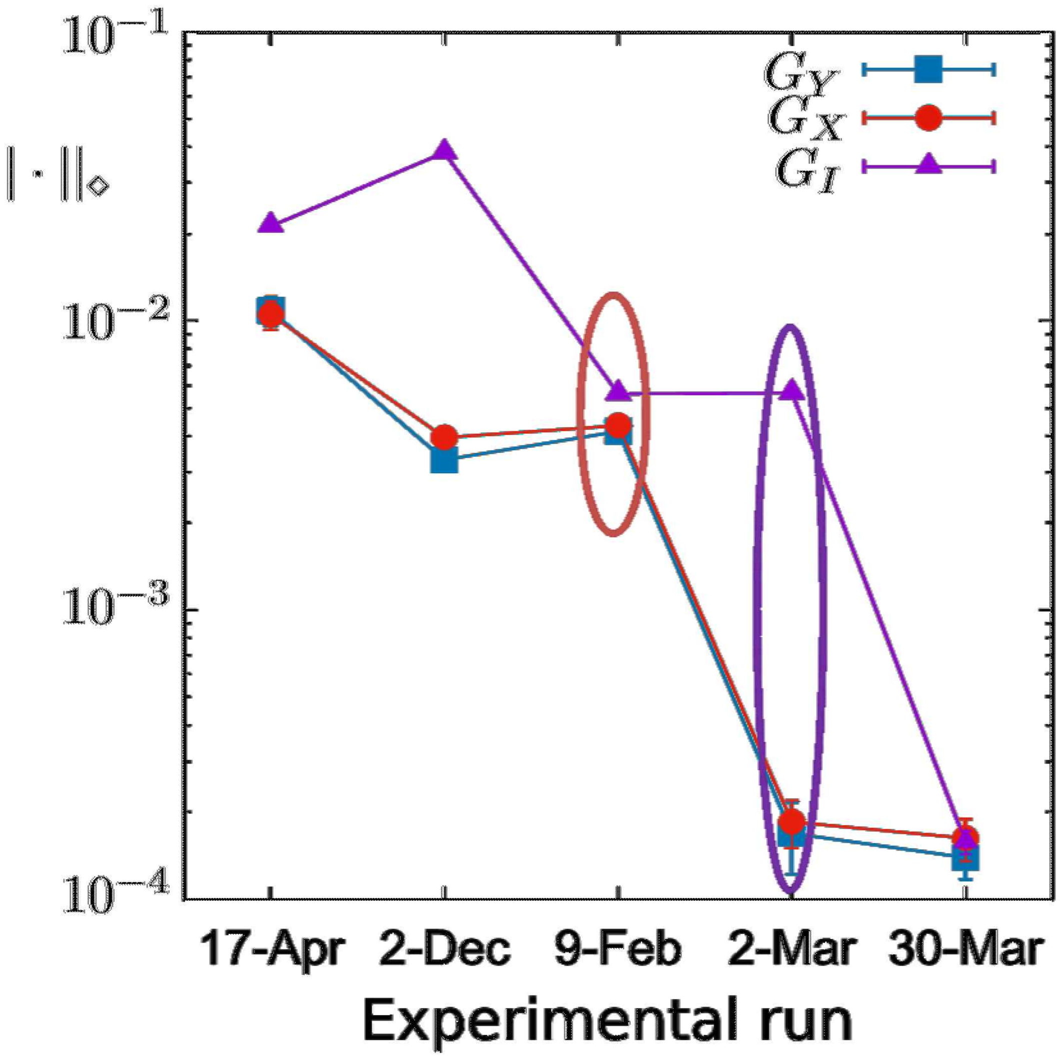

Microwave gates

Raw data good gates

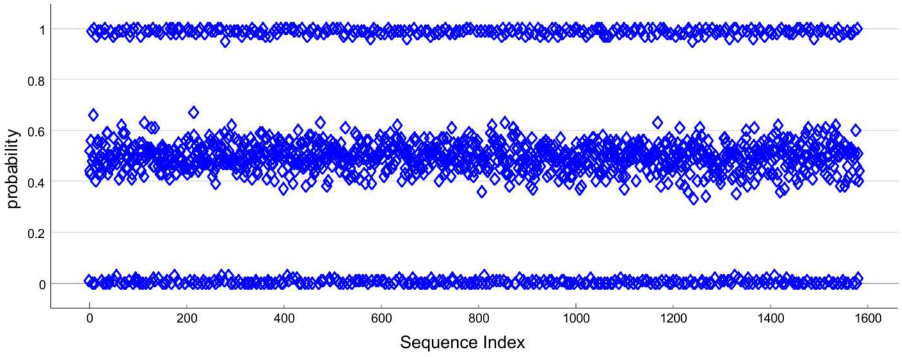

Gate	Rotn. axis	Angle
G_I	-0.0035 0.014 -0.9999 0.0006	0.001769π
G_X	-3×10^{-5} -1 1×10^{-4} 0.0006	0.500007π
G_Y	0.1104 4×10^{-5} 0.9939 0.0005	0.50001π

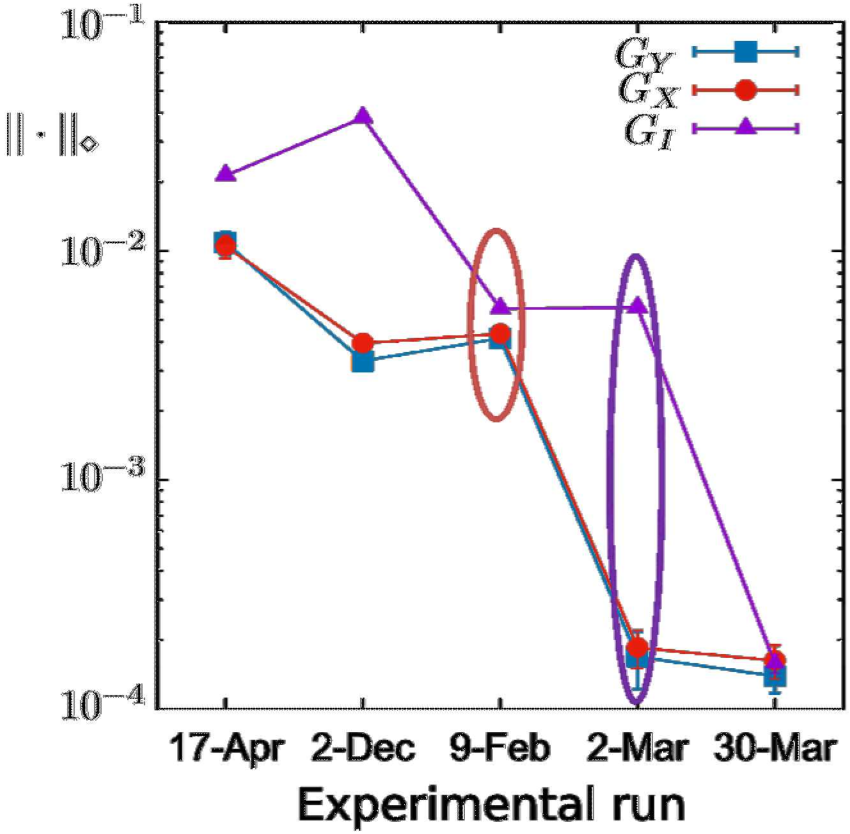

Microwave error sources

- Time resolution:
  - Current time resolution is 5 ns
  - π-times are 45 μs
  - ratio: 10^{-4}
  - Possible due to broadband pulses
- Coherence time:
  - $T_2^* = 1\,\text{s}$
  - longest pulse sequences 8192 : 1.66 s

Single qubit gates
Markovianity violation

- BB1 decoupled microwave gates with decoupled identity have very small non-Markovian noise
- BB1 dynamically compensated pulse sequences
- Decoupling sequence for identity gate
- Drift control for π-time and qubit frequency

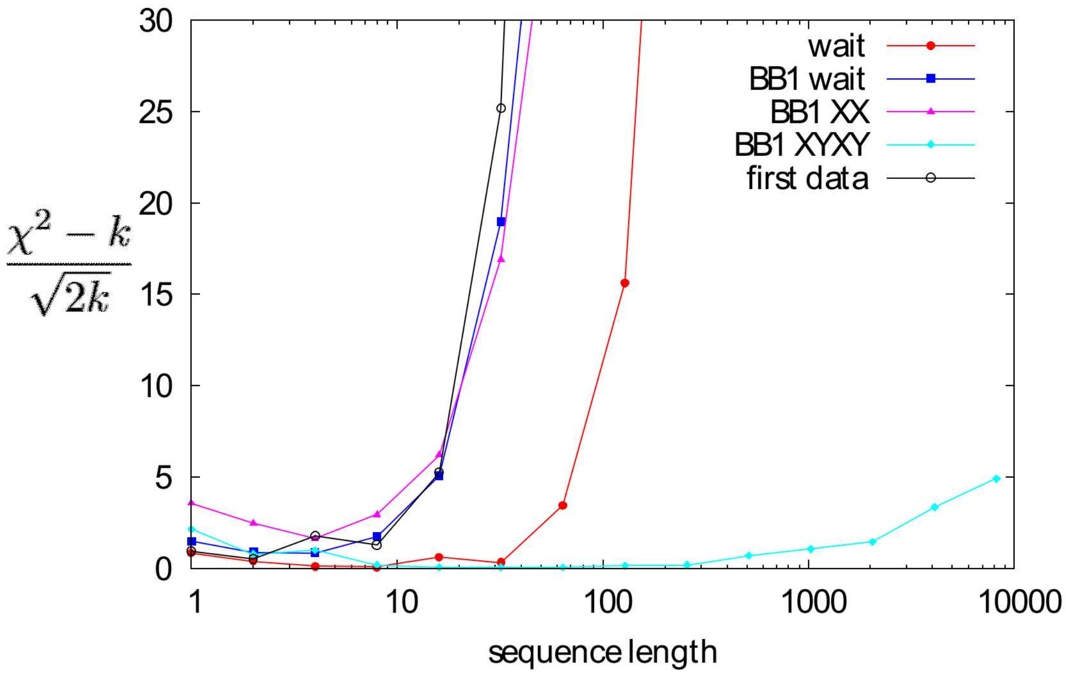

Gate	Process Infidelity	½ ◇-Norm
G_I	$6.9(6) \times 10^{-5}$	$7.9(7) \times 10^{-5}$
G_X	$6.1(7) \times 10^{-5}$	$7.0(15) \times 10^{-5}$
G_Y	$7.2(7) \times 10^{-5}$	$8.1(15) \times 10^{-5}$

95% confidence intervals

R. Blume-Kohout, et al. arXiv:1605.07674 (2016)

Microwave broadband pulses

BB1 compensated pulse

Switching artifacts

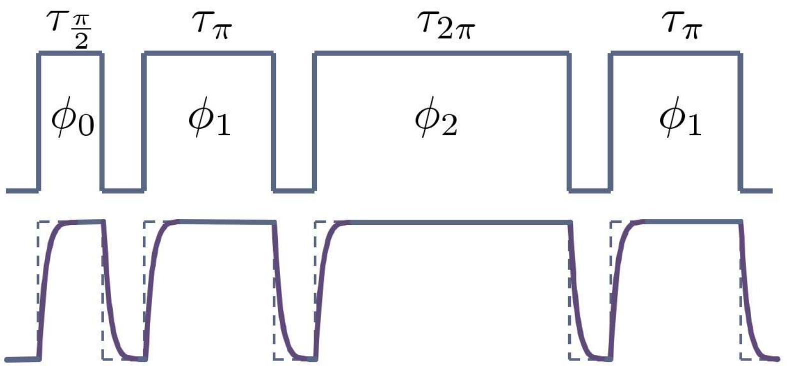

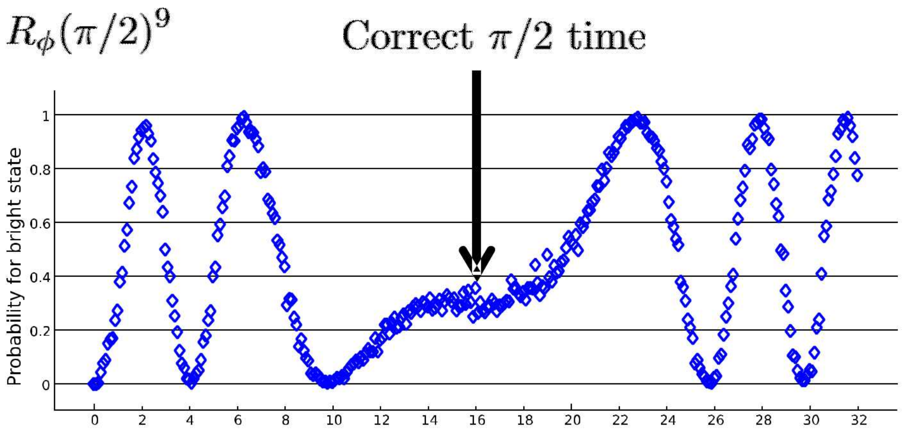

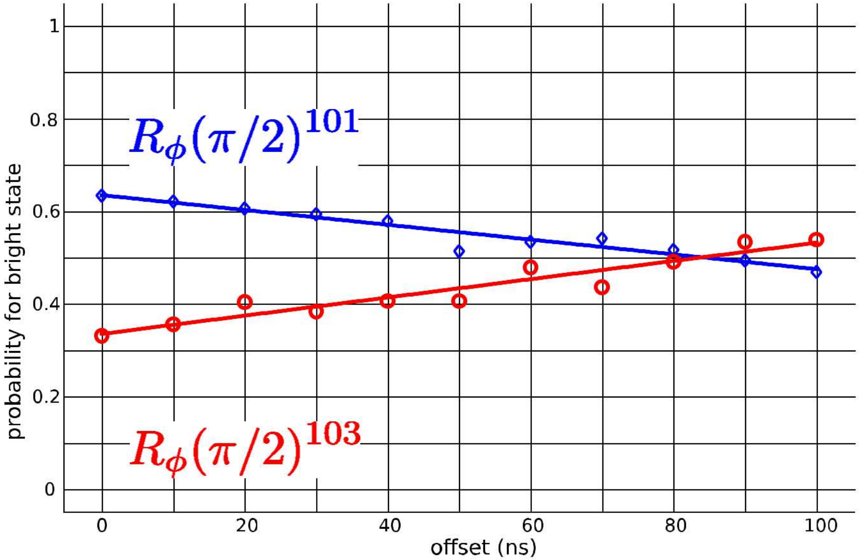

Discontinuous phase updates are used in place of gaps. Solves issues related to finite turn-on time and allows for continuous feedback on the driving field power.

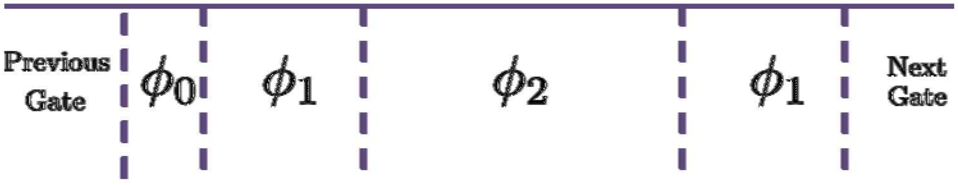

Single qubit gates
Laser based Raman gates

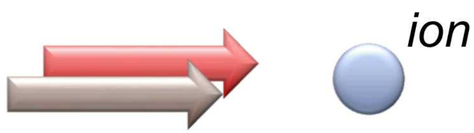

co-propagating beam geometry
- Motion independent
- No optical phase imprinted

- BB1 dynamically compensated pulse sequences

GST results:

95% confidence intervals

	Conventional pulses		Gapless pulses	
Gate	Process Infidelity	1/2 ◇-Norm	Process Infidelity	1/2 ◇-Norm
G_I	$0.05(2) \times 10^{-4}$	$12(1) \times 10^{-4}$	$1.1(1) \times 10^{-4}$	$5.3(2) \times 10^{-4}$
G_X	$1.3(1) \times 10^{-4}$	$4(2) \times 10^{-4}$	$0.5(1) \times 10^{-4}$	$2(6) \times 10^{-4}$
G_Y	$1.6(4) \times 10^{-4}$	$4(3) \times 10^{-4}$	$0.7(1) \times 10^{-4}$	$4(9) \times 10^{-4}$

Mølmer-Sørensen gates

- Mølmer-Sørensen gates [1]
- All two-qubit gates implemented using Walsh compensation pulses [2]

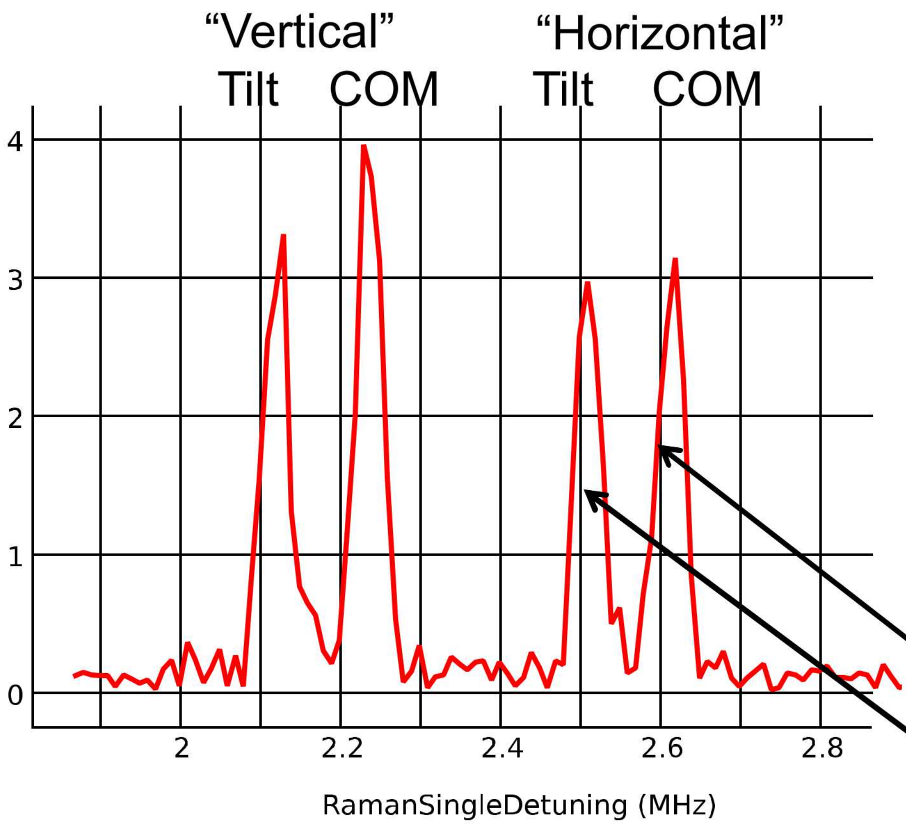

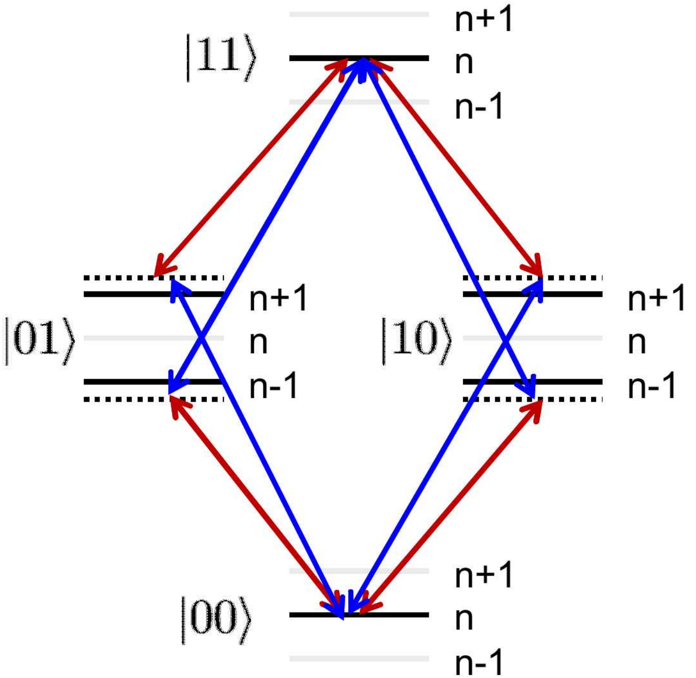

$$|00\rangle \rightarrow |00\rangle + |11\rangle$$

Heating rates

$\approx 60\ ^{\text{quanta}}/_{\text{s}}$

$< 8\ ^{\text{quanta}}/_{\text{s}}$

[1] K. Mølmer, A. Sørensen, PRL 82, 1835 (1999)
[2] D. Hayes et al. Phys. Rev. Lett. 109, 020503 (2012)

Fidelity measurement using parity scan

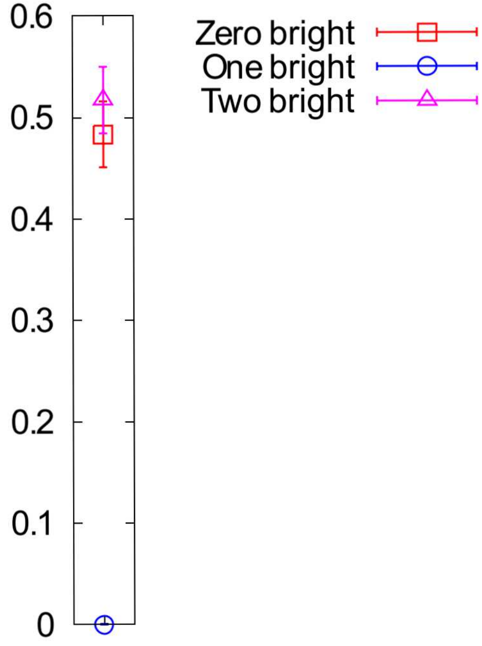

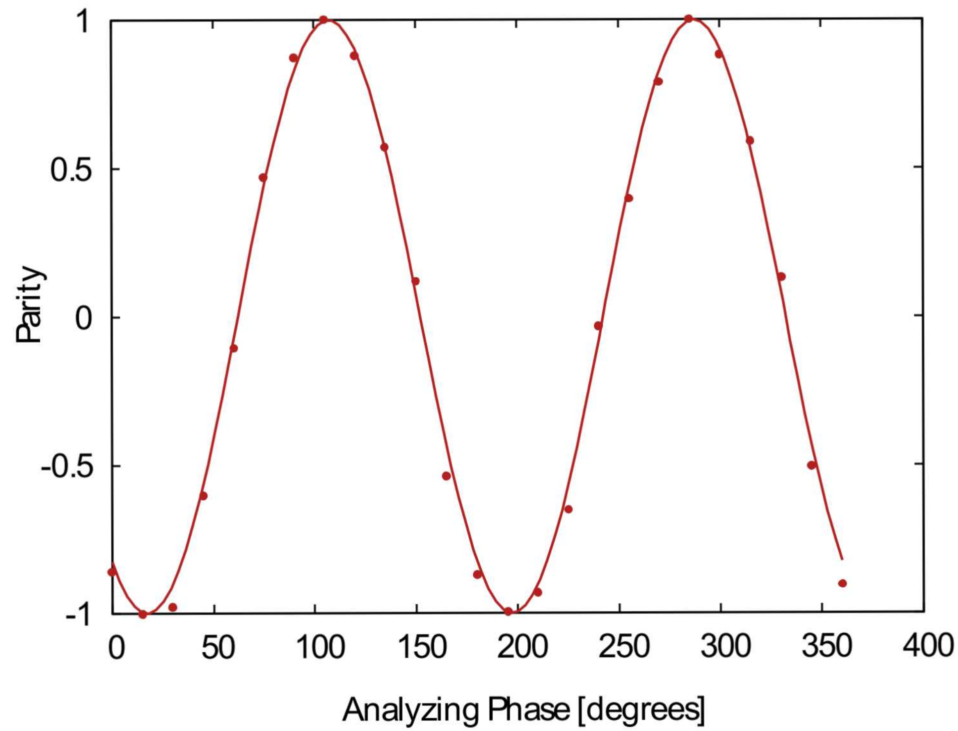

$$\mathcal{F} = \frac{1}{2}(P(|00\rangle) + P(|11\rangle)) + \frac{1}{4}c \approx 0.995$$

Two qubit gates
GST on symmetric subspace

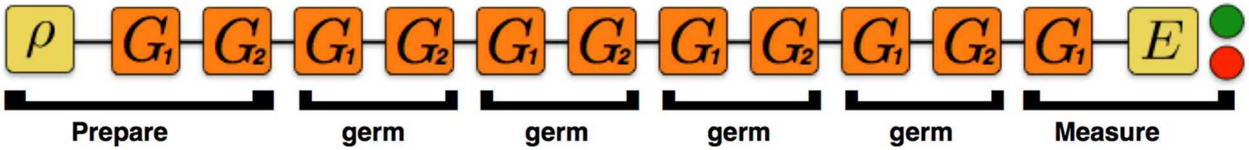

Basic gates:

$$G_I$$

$$G_{XX} = G_X \otimes G_X$$

$$G_{YY} = G_Y \otimes G_Y$$

$$G_{MS}$$

Preparation Fiducials:

$\{\}$

G_{XX}

G_{YY}

G_{MS}

$G_{XX}G_{MS}$

$G_{YY}G_{MS}$

Germs:

G_I

G_{XX}

G_{YY}

G_{MS}

$G_I G_{XX}$

$G_I G_{YY}$

$G_I G_{MS}$

$G_{XX}G_{YY}$

$G_{XX}G_{MS}$

$G_{YY}G_{MS}$

$G_I G_I G_{XX}$

$G_I G_I G_{YY}$

Detection Fiducials:

$\{\}$

G_{XX}

G_{YY}

G_{MS}

$G_{XX}G_{MS}$

$G_{YY}G_{MS}$

G_{XX}^3

G_{YY}^3

$G_{YY}^2 G_{MS}$

Two qubit gates
GST data

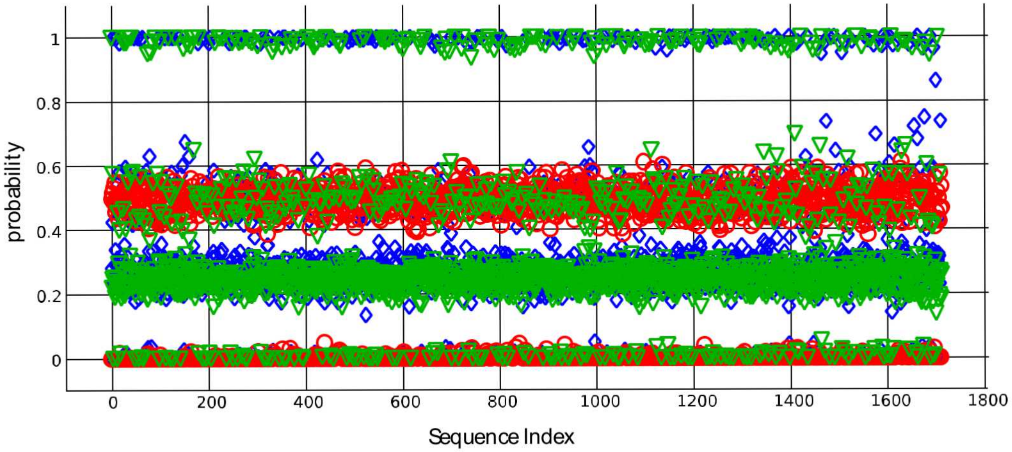

Zero ions bright

One ion bright

Two ions bright

Gate	Process infidelity	$\frac{1}{2}$ Diamond norm
G_I	$1.6 \times 10^{-3} \pm 1.6 \times 10^{-3}$	$28 \times 10^{-3} \pm 7 \times 10^{-3}$
G_{XX}	$0.4 \times 10^{-3} \pm 1.0 \times 10^{-3}$	$27 \times 10^{-3} \pm 5 \times 10^{-3}$
G_{YY}	$0.1 \times 10^{-3} \pm 0.9 \times 10^{-3}$	$26 \times 10^{-3} \pm 4 \times 10^{-3}$
G_{MS}	$4.2 \times 10^{-3} \pm 0.6 \times 10^{-3}$	$38 \times 10^{-3} \pm 5 \times 10^{-3}$

95% confidence intervals

Process fidelity of two-qubit Mølmer-Sørensen gate > 99.5%

Microwave trap

"Ideal" Two-Loop Design

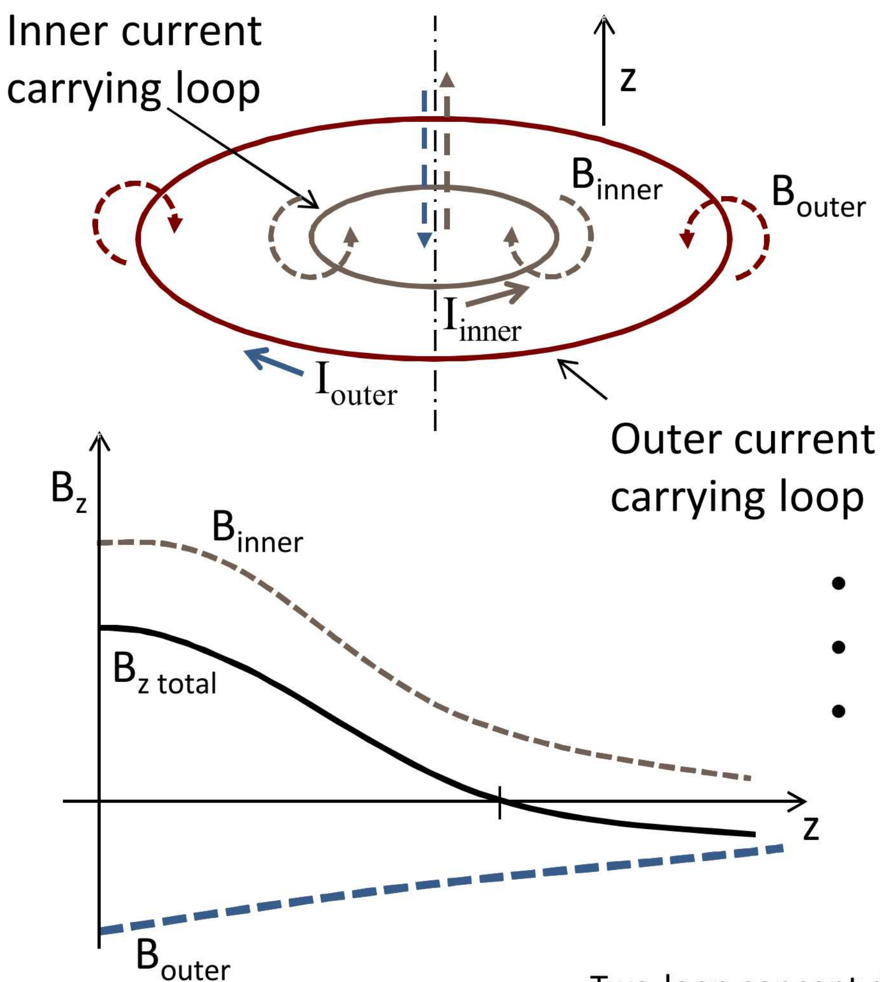

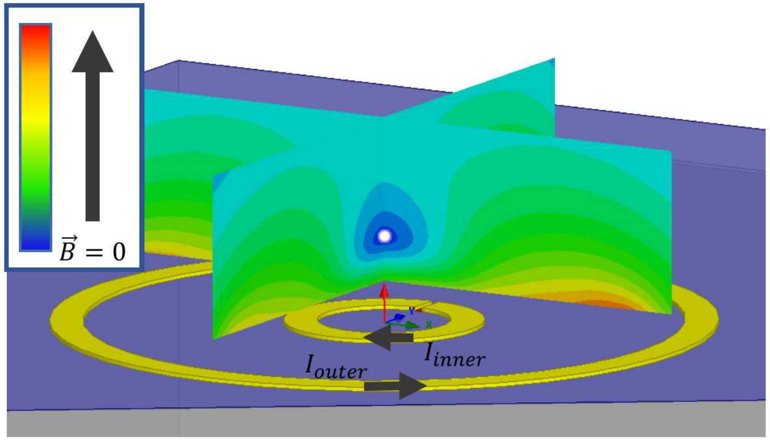

- x- and y- fields cancel along z-axis
- Generates uniform B_z and dB_z/dz with B=0
- Location of null determined by geometry and ratio of currents

Two-loop concept developed at Sandia in 2012 (SAND2015-9513)
(C. Highstrete, S. M. Scott, J. D. Sterk, C. D. Nordquist, J. E. Stevens, C. P. Tigges, M. G. Blain)

Specialized devices & Future directions

Microwave trap

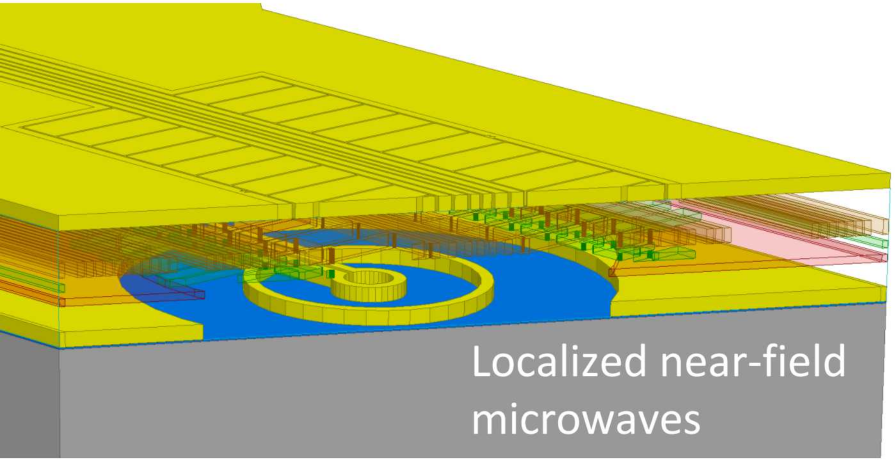

Localized near-field microwaves

Benefits:

- Microwave radiation is easier to control and cheaper to implement than lasers
- Low power for Rabi oscillations
- Near field allows to generate microwave gradient fields

Challenges:

- Microwave delivery
- Dissipation, heating, thermal management

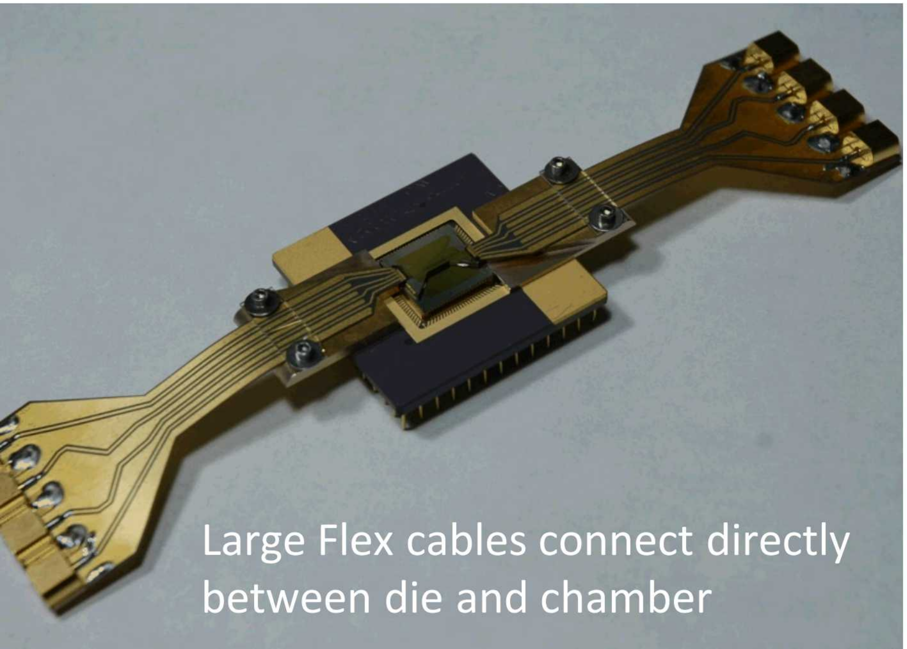

Large Flex cables connect directly between die and chamber

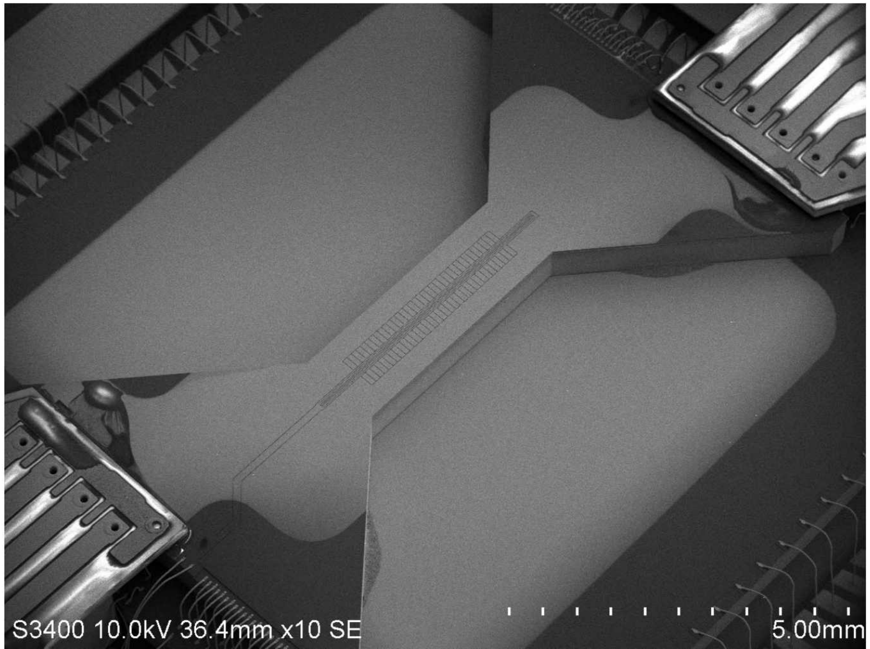

Microwave trap

- Losses between chamber and device ≈17dB
- Realized fast Rabi flopping 330ns with 15dBm at chamber, -2dBm at device
- Access to range of relevant π-times
- Will characterize gates as function of π-times.

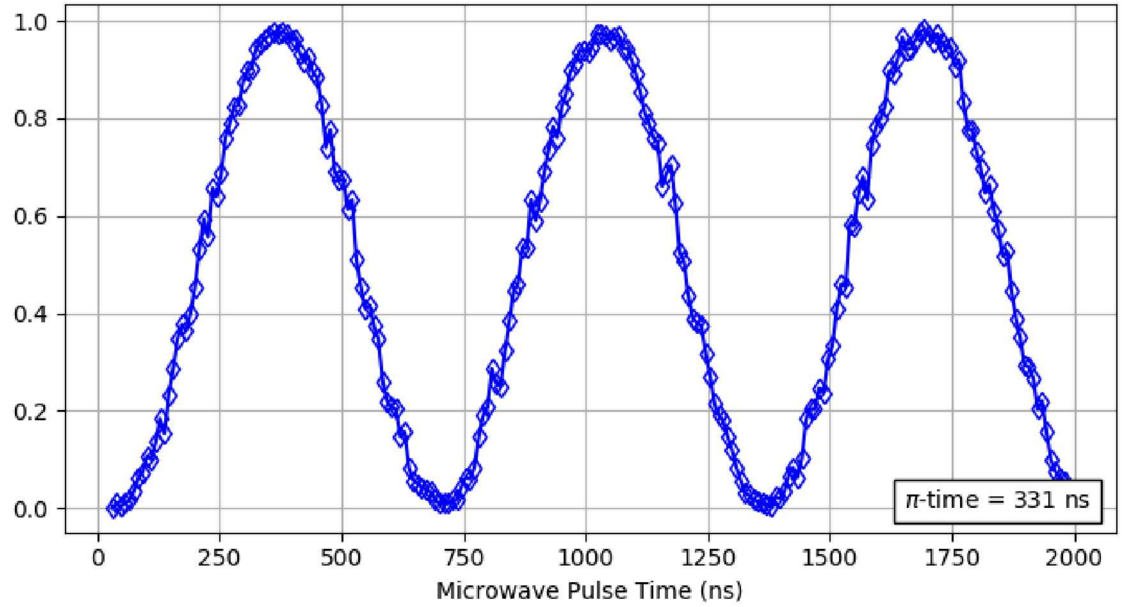

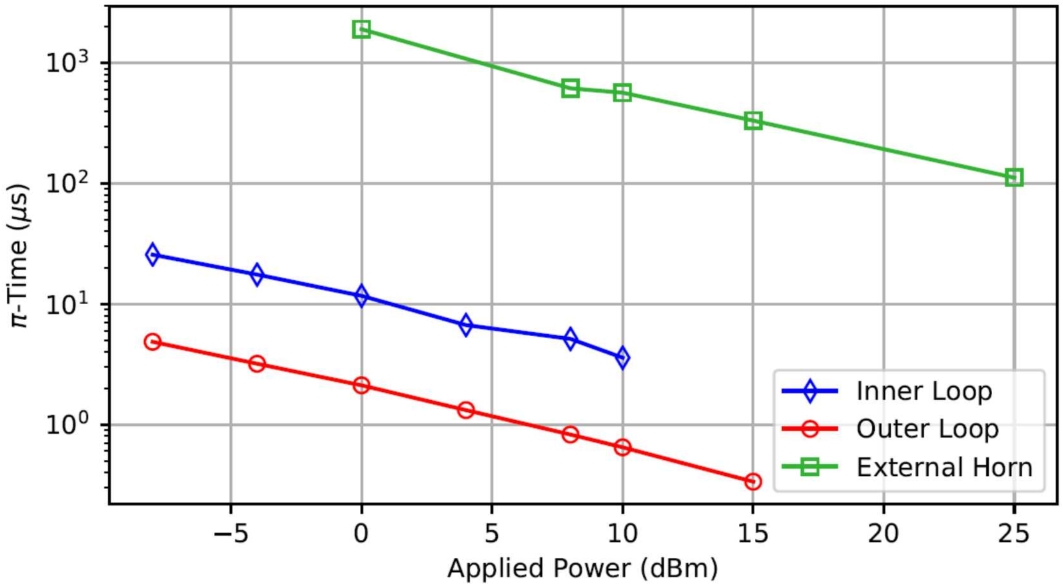

EPICS Trap

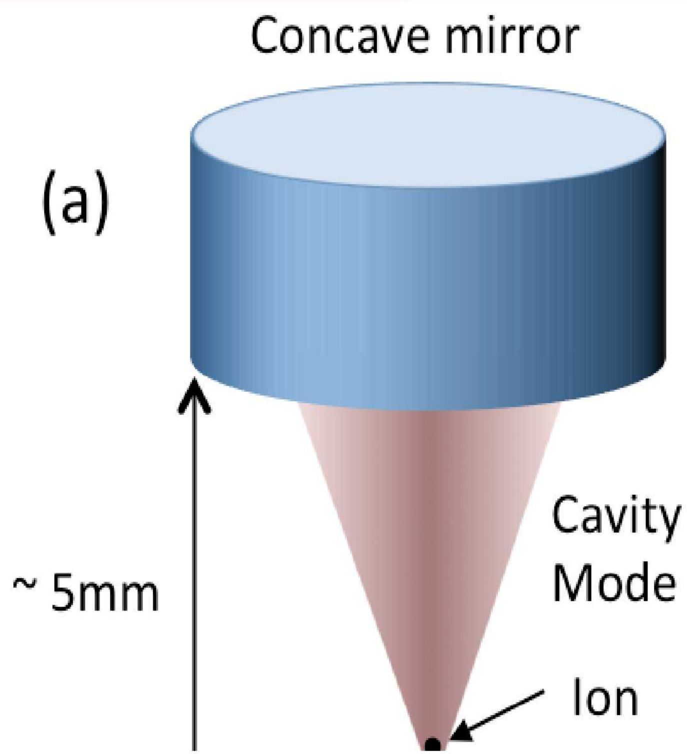

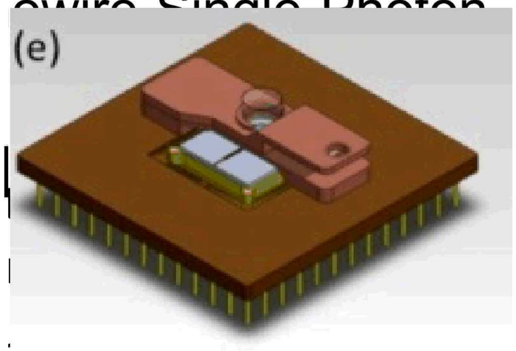

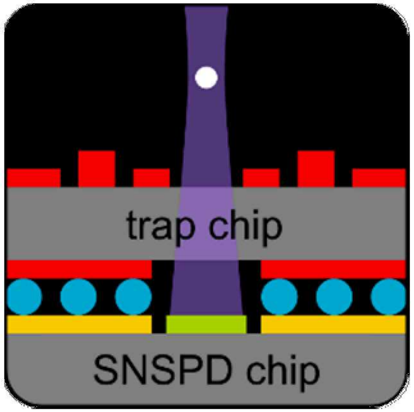

ment

i
ser

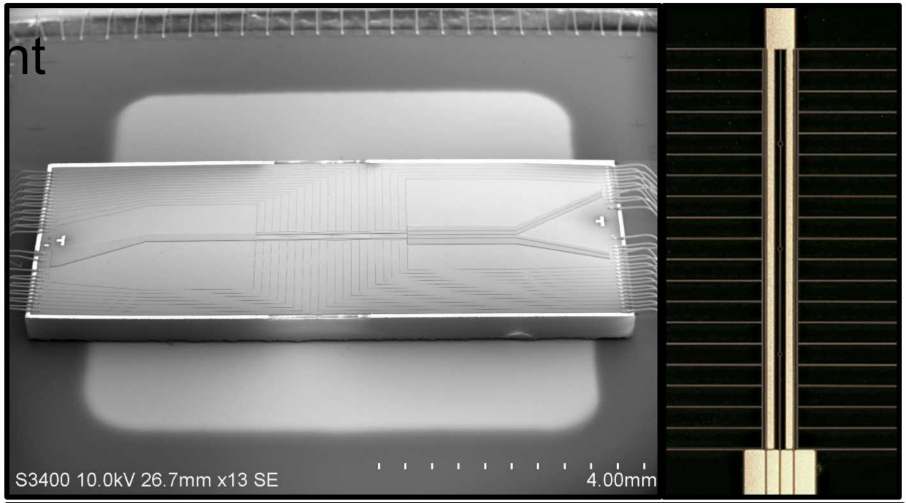

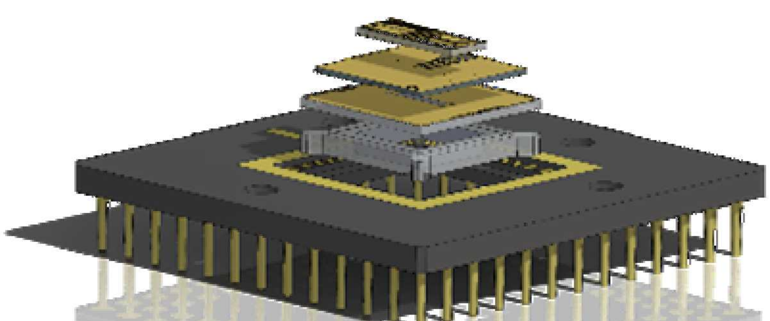

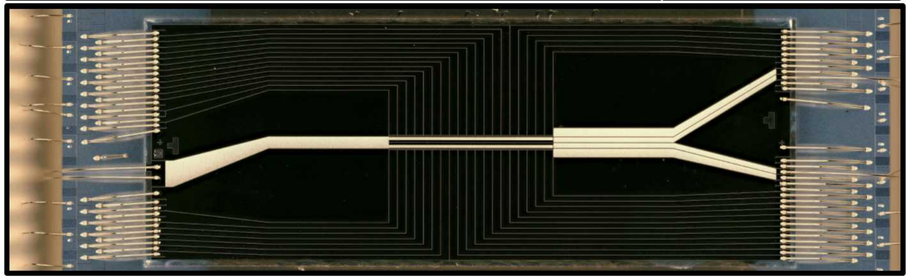

collaboration with

NIST National Institute of Standards and Technology U.S. Department of Commerce

JPL Jet Propulsion Laboratory

Duke University